A&A 465, 993–1002 (2007)
DOI: 10.1051/0004-6361:20066401

Astronomy & Astrophysics

Spectral atlas of massive stars around He I 10 830 Å⋆,⋆⋆,⋆⋆⋆

J. H. Groh[1], A. Damineli[1], and F. Jablonski[2]

[1] Instituto de Astronomia, Geofísica e Ciências Atmosféricas, Universidade de São Paulo, Rua do Matão 1226, Cidade Universitária, 05508-900 São Paulo, SP, Brasil
e-mail: groh@astro.iag.usp.br
[2] Instituto Nacional de Pesquisas Espaciais/MCT, Avenida dos Astronautas 1758, 12227-010 São José dos Campos, SP, Brasil

Received 14 September 2006 / Accepted 8 November 2006

ABSTRACT

We present a digital atlas of peculiar, high-luminosity massive stars in the near-infrared region (10 470–11 000 Å) at medium resolution ($R \simeq 7000$). The spectra are centered around He I 10 830 Å, which is formed in the wind of those stars, and is a crucial line to obtain their physical parameters. The instrumental configuration also sampled a rich variety of emission lines of Fe II, Mg II, C I, N I, and Pa γ. Secure identifications for most spectral lines are given, based on synthetic atmosphere models calculated by our group. We also propose that two unidentified absorption features have interstellar and/or circumstellar origin. For the strongest one (10 780 Å) an empirical calibration between $E(B-V)$ and equivalent width is provided. The atlas displays the spectra of massive stars organized in four categories, namely Be stars, OBA Iape (or luminous blue variables, LBV candidates and ex/dormant LBVs), OB supergiants and Wolf-Rayet stars. For comparison, the photospheric spectra of non emission-line stars are presented. Selected LBVs were observed in different epochs from 2001 to 2004, and their spectral variability reveals that some stars, such as η Car, AG Car and HR Car, suffered dramatic spectroscopic changes during this time interval.

Key words. atlases – stars: emission-line, Be – stars: Wolf-Rayet – stars: winds, outflows – stars: early-type

1. Introduction

In the last decades tremendous progress has been achieved in understanding how a massive star evolves along the HR diagram. A new scenario of massive star evolution was developed after the models allowed for the effects of rotation in the stellar structure and evolution (Maeder & Meynet 2000b). Also, the physical parameters of massive stars can currently be constrained with the advent of a new generation of fully-blanketed, spherical-symmetric, non-LTE radiative transfer codes (Hubeny & Lanz 1995; Hillier & Miller 1998; Hamann & Koesterke 1998; Pauldrach et al. 2001; Gräfener et al. 2002; Puls et al. 2005). Even for extremely massive objects such as Eta Carinae (Hillier et al. 2001) we now have a much better comprehension of the physical parameters of the central star by analyzing the emerged spectrum.

However, the short transitional stages of massive star evolution are still poorly understood. The radiation emitted by the photosphere of these stars interacts with the optically-thick, dense wind, which makes the spectral classification a very challenging task. In addition to the luminosity, effective temperature and surface gravity, several other stellar parameters might change the spectral morphology of these objects, notably the mass-loss rate and the wind terminal velocity. In the discussion on the characteristics of the atlas, we point out the similarities and differences in the spectral morphology of massive stars belonging to different evolutionary stages.

The aim of this paper is to extend the idea of the *OB Zoo* published by Walborn & Fitzpatrick (2000, hereafter WF2000) to the near-infrared region of the spectrum. Some of the objects present in this work were observed at lower resolution from 1.0 to 2.5 μm by McGregor et al. (1988). In addition, peculiar massive stars were also observed around 8500 Å and 10 000 Å by Lopes et al. (1992), and in the *H* and *K* bands by Morris et al. (1996).

We chose to explore the "forgotten" region around He I 10 830 Å due to the strength of this line, which is often the strongest one in the near-infrared region. Pioneering observations of early-type stars around this line were published by Andrillat & Vreux (1979) and by Meisel et al. (1982). Especially for objects with dense winds and high terminal velocities, He I 10 830 Å is one of the few strong He I lines that is unblended. This line is formed over a large region of the wind and thus it is a crucial diagnostic of the physical properties of the wind and of the underlying photosphere. Moreover, with a relatively short spectral coverage around 10 830 Å, we can sample a number of strong, unblended lines, such as Pa γ, and rich emission-line spectra of Fe II, Mg II, C I, and N I. They provide important constraints on the physical conditions found in those stars and their winds.

We observed other peculiar objects that are not present in WF2000, but are as fascinating and intriguing as their original program stars. Meanwhile, we did not observe some objects present in WF2000, especially the faintest ones, that were beyond the limiting magnitude of our instrumental configuration. Nevertheless, we tried to cover a large range of evolutionary

⋆ Based on observations made at Observatório do Pico dos Dias/LNA (Brazil).
⋆⋆ Figures 5 to 18 are only available in electronic form at http://www.aanda.org
⋆⋆⋆ Electronic version of the spectra (fichiers FITS) is only available in electronic form at the CDS via anonymous ftp to cdsarc.u-strasbg.fr (130.79.128.5) or via http://cdsweb.u-strasbg.fr/cgi-bin/qcat?J/A+A/465/993

phases and physical parameters found in hot stars. However, it is beyond the scope of this paper to present a full evolutionary sequence of massive stars around 10 830 Å, especially considering that a significant fraction of the objects shown here does not have a well-determined evolutionary stage.

As part of the atlas, we present the spectral variability of a large sample of luminous blue variables (henceforth LBV) and LBV candidates during a time interval of 3 yr. To the best of our knowledge, this is the first work in any spectral region to present the spectroscopic variability on a timescale of a few years (which is typical for S Dor-type variations), for a large sample of LBVs and related objects. As we show along the atlas, different behaviors of variability can be noticed (radial velocity, line profile, strength).

This paper is organized as follows. In Sect. 2 we describe the observations made at the Observatório Pico dos Dias (LNA/Brazil); in Sect. 3 we present the atlas, briefly contextualizing and introducing each class of objects, and then describing the past bibliography and the spectral features of each individual object. In Sect. 4 we discuss the unidentified features present in the program stars.

2. Observations

The near-infrared spectra were obtained using a HgCdTe 1024 × 1024 infrared array (CamIV) mounted on the Coudé focus of the 1.6 m telescope at the Observatório do Pico dos Dias/LNA (Brazil). The stars were observed on 2001 June 09−12, and again on 2004 April 30 and 2004 July 02−04. Spectra of variable stars were also taken on 2002 November 04, and 2003 June 28.

For each object, we combined up to 35 individual exposures varying between 10 s and 60 s to reach typically $S/N = 80$ in the continuum. We used a 600 gr/mm grating and a 1-arcsec slit width to obtain $R \simeq 7000$ and 0.64 Å/pixel of dispersion, covering the spectral range of 10 470−11 000 Å. The sky+thermal background subtraction was accomplished by dithering the star along the slit in 7 positions. We median-combined these 7 frames to obtain a median sky image, which was then subtracted from each original frame. Each sky-subtracted image was then divided by a normalized flat-field image. The following data reduction, extraction of the spectrum and analysis was made by using usual IRAF routines. The wavelengths were calibrated using an internal ThAr emission lamp, achieving a typical rms uncertainty of 0.08 Å (∼2.2 km s^{-1}). The telluric features were removed from the program stars' spectra by dividing them by the spectrum of a fast-rotating hot star. The photospheric Pa γ and He I 10 912 Å absorptions were previously removed from the fast-rotating star by interpolating the adjacent continuum with a low-order Legendre polynomial. The extracted spectra were corrected to the heliocentric frame and normalized to the continuum intensity using a low-order Legendre polynomial (errors in normalization are typically 1%). No flux calibration or de-reddening was done.

3. The atlas

The atlas consists of 10 figures, containing from two to six spectra of hot luminous stars each, thus 40 peculiar objects. The spectral evolution of selected objects during 2001−2004 is shown in Figs. 16 to 18. An additional figure (Fig. 15) contains the spectra of normal early-type stars, to be used as a reference for the characteristic photospheric features. Each figure shows the air wavelength in Å versus the normalized intensity, plus an arbitrary offset, except where indicated otherwise. Some figures were resampled to show only the region that has strong spectral lines for a given group of stars. The peculiar objects were grouped based on their spectroscopic characteristics, and the basic data of these stars are presented in Table 1.

Many stars have been extensively studied in other spectral regions, whilst some of them have very scarce recent bibliography. Compared to the previous published data in this spectral region, the higher resolution and higher *S/N* of our spectra allowed us to identify many faint spectral lines. They were identified by comparing the value of the oscillator strength of the transition with the observed line intensities, and then checking for the presence of lines of the same multiplet or ionization stage in other wavelength regions (e.g. optical). Almost all the identifications were confirmed by comparing the observations with synthetic spectra (Groh et al. 2007, in preparation), using the radiative transfer code CMFGEN (Hillier & Miller 1998). However, there are still unidentified spectral features remaining, which will be discussed in Sect. 4. In Table 2 we summarize the detected features in the spectra of the program stars; the air wavelengths were taken from the Atomic Line List v2.04[1]. The line identifications are overploted on the spectrum of the LBV AG Carinae taken in 2004 April (Fig. 1).

The atlas is organized as follows: in Sect. 3.1 we present the spectra of the Be stars, in Sect. 3.2 we show the spectra of the LBVs and LBV candidates, in Sect. 3.3 we group the OB supergiants, and in Sect. 3.4 the spectra of the Wolf-Rayet stars. In each subsection we briefly introduce the general characteristics of the class, and discuss the relevant aspects and details of the observed features for each star, comparing them with another objects of our atlas when appropriated.

3.1. The Be stars

The 13 classical Be stars of our sample are shown in decreasing order of spectral type in Figs. 5−7. Most stars in this class show Fe II lines, He I 10 830 Å and Pa γ in emission, often double-peaked. The sole exception is HD 120991, which does not show Fe II lines. Some of the Be stars also show emissions in C I and Mg II lines, that have the same morphology as the Fe II emission.

X Persei (Fig. 7) is a Be/X-ray binary in our sample, such as HD 110432 (Clark et al. 2001). X Persei is the optical counterpart of the pulsar 4U 0352+30 (Clark et al. 2001). The system has a low eccentricity ($e = 0.11$) and a long orbital period of 250 days (Delgado-Martí et al. 2001). Its optical spectrum is characterized by both Hα and He I 6678 Å showing significant variability (Clark et al. 2001). In the near-infrared, its spectrum shows double-peaked emission in Fe II 10 500 Å (−100 and 195 km s^{-1}), while He I 10 830 Å presents a weak double-peaked profile (−98 and 13 km s^{-1}), such as Pa γ (−100 and −5 km s^{-1}). Fe II 10 862 Å is present too, but it is very weak. Mg II lines at 10 915 and 10 952 Å are narrow.

***δ* Scorpii** (Fig. 7) has been claimed to be a classic Be star based on its optical and infrared spectroscopy history, recently undergoing a Hα outburst (Fabregat et al. 2002). However, for many years it was considered a typical B-type star. Previous observations did not show any emission lines (Heasley & Wolff 1983; Grigsby et al. 1992). δ Scorpii is in a highly eccentric binary system, with an orbital period of 10.6 yr (Banerjee et al. 2001). Since the appearance of emission lines coincided with the periastron passage, binarity could be an

[1] http://www.pa.uky.edu/~peter/atomic

Table 1. Basic data for the program stars, ordered by increasing right ascension. Projected rotational velocities are indicated for Be stars, while the presence of a circumstellar nebula is indicated for LBVs and related objects. References are: CN04 = Clark & Negueruela (2004); Cro06 = Crowther et al. (2006); Mir01 = Miroshnichenko et al. (2001); L97 = Lyubimkov et al. (1997); LL06 = Levenhagen & Leister (2006); Riv97 = Rivinius et al. (1997); R97 = Roche et al. (1997); S06 = Smith & Balona (2006); Sta03 = Stahl et al. (2003); vG92 = van Genderen et al. (1992); vG01 = van Genderen (2001); WF2000 = Walborn & Fitzpatrick (2000); Z05 = Zorec et al. (2005).

Be stars

Name	HD	RA (J2000)	Dec (J2000)	Spectral type	$v \sin i$ (km s^{-1})	Reference	Fig.	Obs. Date
X Per	24534	03 55 23.1	+31 02 45.0	B0Ve	293	L97, R97, Z05	7	02 Nov. 04
β Mon A	45725	06 28 49.4	–07 02 03.5	B3Ve	330	Z05	7	02 Nov. 04
δ Cen	105435	12 08 21.5	–50 43 20.7	B2Vne	240	LL06	6	01 Jun. 09
HD 110432	110432	12 42 50.3	–63 03 31.0	B1IVe	300	S06	7	02 May 01
HD 120991	120991	13 53 57.2	–47 07 41.4	B2Ve	130	LL06	6	01 Jun. 09
η Cen	127972	14 35 30.4	–42 09 28.2	B2Ve	310	LL06	5	01 Jun. 09
HD 142983	142983	15 58 11.4	–14 16 45.7	B3IVe	390	Z05	5	01 Jun. 09
δ Sco	143275	16 00 20.0	–22 37 18.2	B0.3IVe	150	Mir01	7	02 Apr. 29
χ Oph	148184	16 27 01.4	–18 27 22.5	B1.5Ve	144	Z05	6	01 Jun. 12
α Ara	158427	17 31 50.5	–49 52 34.1	B2Vne	270	LL06	5	01 Jun. 09
66 Oph	164284	18 00 15.8	+04 22 07.0	B2Ve	220	LL06	5	01 Jun. 09
λ Pav	173948	18 52 13.0	–62 11 15.3	B2IIIe	140	Z05	7	02 Apr. 29
υ Cyg	202904	21 17 55.1	+34 53 48.8	B2 Ve	185	Z05	6	01 Jun. 10

LBVs, LBV candidates and ex/dormant LBVs

Name	HD	RA (J2000)	Dec (J2000)	Spectral type	Nebula	Reference	Fig.	Obs. Date(s)
HD 87643	87643	10 04 30.3	–58 39 52.1	Bpec	yes	WF2000	11	01 Jun. 12
HR Car	90177	10 22 53.8	–59 37 28.4	B3Ia–A2Ia	yes	WF2000, vG01	8, 18	01 Jun. 12, 04 Apr. 30
η Car	93308	10 45 03.6	–59 41 03.3	Bpec	yes	WF2000, vG01	9, 17	01 Jun. 12, 02 Nov. 04, 03 Jun. 28, 04 Apr. 30
GG Car	94878	10 55 58.0	–60 23 33.4	Bpec	no	WF2000	11	01 Jun. 12
AG Car	94910	10 56 11.6	–60 27 12.8	WN11h–Apec	yes	WF2000, vG01	10, 16	01 Jun. 09, 02 Nov. 04, 04 Apr. 30, 04 Jul. 02
He 3-519	–	10 53 59.6	–60 26 44.3	WN11h	yes	WF2000, vG01	9, 17	01 Jun. 12, 04 Apr. 30
W 243	–	16 47 07.5	–45 52 28.5	A2Ia	no	CN04	8	04 Jul. 02
HD 326823	326823	17 06 53.9	–42 36 39.7	Bpec	no	WF2000	11	01 Jun. 12
HD 160529	160529	17 41 59.0	–33 30 13.7	A2Ia	no	Sta03	8, 18	01 Jun. 12, 04 Apr. 30
HD 316285	316285	17 48 14.0	–28 00 53.5	Bpec	no	WF2000	9, 17	01 Jun. 09, 02 Nov. 04, 04 Apr. 30
HD 168607	168607	18 21 14.7	–16 22 32.1	B9Iape	no	WF2000	8, 18	01 Jun. 09, 04 Jul. 02
HD 168625	168625	18 21 19.5	–16 22 26.0	B6Iap	yes	WF2000	8, 18	01 Jun. 09
MWC 314	–	19 21 34.0	+14 52 56.9	Bpec	no	vG01, Mir03	10, 16	01 Jun. 09, 02 Nov. 04, 04 Apr. 30, 04 Jul. 02
P Cyg	193237	20 17 47.2	+38 01 58.5	Bpec	yes	WF2000, vG01	10, 16	01 Jun. 10, 02 Nov. 04, 04 Jul. 02

OB Supergiants

Name	HD	RA (J2000)	Dec (J2000)	Spectral type	Reference	Fig.	Obs. Date(s)
HD 80077	80077	09 15 54.8	–49 58 24.6	B2Ia+	vG92, vG01	12	01 Jun. 12
HD 151804	151804	16 51 33.7	–41 13 49.9	O8Iaf	WF2000	12	01 Jun. 09
WR 79a	152408	16 54 58.5	-41 09 03.1	O8:Iafpe,WN9ha	WF2000	12	01 Jun. 09
ζ^1 Sco	152236	16 53 59.7	–42 21 43.3	B1.5Ia+	Cro06	12, 18	01 Jun. 11, 04 Jul. 02
HD 154090	154090	17 04 49.3	–34 07 22.5	B0.7Ia	Cro06	12	01 Jun. 09, 04 Jul. 02
HD 169454	169454	18 25 15.1	–13 58 41.5	B1Ia+	Riv97	12, 18	01 Jun. 09, 04 Jul. 02

Wolf-Rayet stars

Name	HD	RA (J2000)	Dec (J2000)	Spectral type	Reference	Fig.	Obs. Date(s)
WR 6	50896	06 54 13.0	–23 55 42.0	WN4	vdH01	13	02 Nov. 04
WR 11	68273	08 09 32.0	–47 20 11.7	WC8+O7.5III-V	vdH01	14	01 Jun. 11
WR 22	92740	10 41 17.5	–59 40 36.9	WN7h+O9III-V	vdH01	13	01 Jun. 09
WR 78	151932	16 52 19.2	–41 51 16.2	WN7h	vdH01	13	01 Jun. 09
WR 90	156385	17 19 29.9	–45 38 23.9	WC7	vdH01	14	01 Jun. 11
WR 103	164270	18 01 43.1	–32 42 55.2	WC9d	vdH01	14	01 Jun. 11
WR 136	192163	20 12 06.5	+38 21 17.8	WN6(h)	vdH01	13	01 Jun. 09

alternative hypothesis to explain the Be phenomenon in this object (Fabregat et al. 2000; Miroshnichenko et al. 2001). In our near-infrared spectrum δ Scorpii shows double-peaked Fe II 10 500 Å and 10 862 Å (−65 and +130 km s^{-1} and −45 and +80 km s^{-1}, respectively). C I 10 683, 10 685 and 10 691 Å (blend), C I 10 707 Å, and C I 10 729 Å are present in emission. The He I 10 830 Å line is strong, while Pa γ is weak. The Mg II lines are broad and may be double-peaked.

Table 2. Observed line transitions in the program stars.

Ion	λ_{air} (Å)	Identification
Fe II	10 485.940	$e^6D_{5/2}-{}^6D^0_{5/2}$
Fe II	10 490.942	$z^4F_{7/2}-b^4G_{7/2}$
Fe II	10 499.297	$z^4F_{7/2}-b^4G_{5/2}$
Fe II	10 501.499	$z^4F_{7/2}-b^4G_{9/2}$
N I	10 507.000	$^4P^0_3-{}^4D_5$
N I	10 513.410	$^4P^0_1-{}^4D_1$
N I	10 520.580	$^4P^0_3-{}^4D_3$
Fe II	10 525.122	$w^2D_{3/2}-{}^4P_{5/2}$
N I	10 533.760	$^4P^0_3-{}^4D_1$
N I	10 539.574	$^4P^0_5-{}^4D_7$
Fe II	10 546.348	$e^6D_{9/2}-y^6F^0_{11/2}$
N I	10 549.640	$^4P^0_5-{}^4D_5$
N I	10 563.330	$^4P^0_5-{}^4D_3$
Fe II	10 591.170	$e^6D_{5/2}-{}^6D^0_{3/2}$
Fe II	10 655.649	$d^2F_{7/2}-z^2F^0_{7/2}$
He I	10 667.65	$3p\,^3P^0-6s\,^3S$
C I	10 683.080	$^3P^0_1-{}^3D_2$
C I	10 685.340	$^3P^0_0-{}^3D_1$
C I	10 691.240	$^3P^0_2-{}^3D_3$
C I	10 707.32	$^3P^0_1-{}^3D_1$
Fe II	10 709.730	$e^6D_{7/2}-y^6F^0_{5/2}$
Fe II	10 711.060	$e^6D_{3/2}-{}^6D^0_{5/2}$
N I	10 713.548	$^4P^0_3-{}^4P_5$
N I	10 717.950	$^4P^0_3-{}^4P_3$
C I	10 729.53	$^3P^0_2-{}^3D_2$
Fe II	10 749.781	$e^6D_{7/2}-y^6F^0_{7/2}$
N I	10 757.887	$^4P^0_5-{}^4P_5$
Fe II	10 820.88	$e^6D_{3/2}-{}^6D^0_{3/2}$
Fe II	10 826.483	$e^6D_{7/2}-y^6F^0_{9/2}$
Fe II	10 829.550	$z^4D_{3/2}-b^4G_{5/2}$
He I	10 830.34	$2s\,^3S-2p\,^3P^0$
Fe II	10 862.644	$z^4F_{5/2}-b^4G_{7/2}$
Fe II	10 871.601	$z^4F_{5/2}-b^4G_{5/2}$
Fe II	10 899.370	$e^6D_{3/2}-y^6F^0_{1/2}$
He I	10 912.99	$3d\,^3D-6f\,^3F^0$
Mg II	10 914.280	$^2D_5-{}^2P^0_3$
He I	10 917.062	$3d\,^1D-6f\,^1F^0$
Pa γ	10 938.095	6–3
Mg II	10 951.770	$^2D_3-{}^2P^0_1$

HD 110432 (Fig. 7) is a Be star that is located just beyond the southern part of the Coalsack at a distance of 300 ± 50 pc (Rachford et al. 2001). It is one of the brightest stars lying behind interstellar material and it has narrow absorption resonance lines in the UV spectrum (Codina et al. 1984; Prinja & Henrichs 1987). The optical data displays line-profile variations from night to night (Codina et al. 1984). Torrejón & Orr (2001) classified HD 110432 as a low luminosity Be/X-ray binary. Its near-infrared spectrum looks like that of δ Scorpii, although we have found a symmetrically double-peaked profile in He I 10 830 Å and in Pa γ, both with peaks at −80 and 80 km s^{-1}. As in δ Centauri, a weak feature was found at 10 541 Å and we identified it as N I 10 539.6 Å.

χ Ophiuchi (Fig. 6) displays fast variability in the Balmer series lines (Doazan 1970). Borisova (1992) observed variations in the He I optical lines with a period of 0.913 day, and suggested

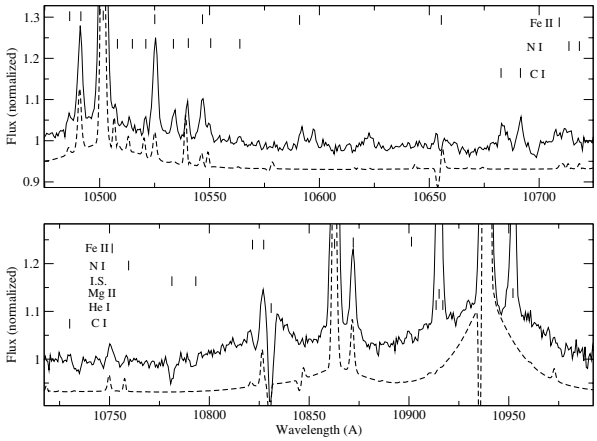

Fig. 1. Identification of the features present in the 2004 April spectrum of the LBV AG Carinae (full line). Thanks to the high resolution and high *S/N* provided by the infrared spectrograph (CamIV) we could identify a number of weak features present in the spectrum. The dashed line shows a non-LTE radiative transfer model for AG Car (Groh et al. 2006, in preparation) which was used to confirm the line identifications. Extended, strong electron-scattering wings are noticeable in He I 10 830 Å and Pa γ, and are present in several other LBVs (see Figs. 8–10).

that χ Oph is a non-radial pulsator. Its near-infrared spectrum is dominated by narrow emissions lines of Fe II, Mg II, C I and Pa γ. The C I lines are more prominent than in the other Be stars of our sample. The He I 10 830 Å emission is weak.

HD 120991 (Fig. 6) is a pole-on Be star that has shown strong and variable emission features since it was first studied by Fleming (1890). The optical H lines show strong profile variations and the Fe II lines show weak V/R variability (Hanuschik et al. 1995; Hanuschik & Vrancken 1996). Its IUE spectrum was first studied by Dachs & Hanuschik (1984), who claimed that most of the resonance lines arise in the interstellar medium. The high excitation resonance lines of N V, C IV, and Si IV do not seem to be formed in a high-velocity expanding envelope (Hubeny et al. 1986). Hence, he concluded that the IUE spectrum of HD 120991 is associated with the stellar photosphere. In the near-infrared spectrum this star presents few narrow emission lines (He I 10 830 Å, Pa γ and Mg II) that have a single-peak profile.

***υ* Cygni** (Fig. 6) is a classical Be star first detected by Fleming (1890). This object shows strong Hα emission (Neiner et al. 2005), variable on different timescales. Outbursts are quite common in this object, such as the one detected by the Hipparcos satellite. In our atlas its spectrum resembles that of δ Centauri, except that the C I lines are stronger, Mg II lines are weaker, and Pa γ is symmetrically double-peaked (−50 and +55 km s^{-1}). The Fe II 10 500 Å and 10 862 Å lines are double-peaked as well (−30 and +115 km s^{-1} and −36 and +77 km s^{-1}, respectively).

66 Ophiuchus (Fig. 5) is a well-observed Be star. Peters (1982) analyzed the first IUE observations and detected high velocity absorption components (from −250 to −850 km s^{-1}) in the resonance lines of C IV, Si IV, and Si III. Based on the UV spectrum, strong variations were detected in its stellar-wind lines (Barker & Marlborough 1985), vanishing and appearing in intervals of several months (Grady et al. 1987). 66 Oph has a long history of optical variability, showing Hα emission with irregular variations. Cyclic V/R variability was also detected in Hα during the period 1982–1993. In our near infrared spectrum 66 Oph shows weak Fe II, C I and He I emission lines. Pa γ

is almost symmetrically double-peaked (violet and red peaks at −110 and +90 km s^{-1}, respectively), reaching up to 0.4 of the continuum intensity (i.e., $F_{\rm peak}/F_{\rm c}$ = 1.4). Pa γ also presents an absorption profile on the blue side that can be P Cygni absorption.

***η* Centauri** (Fig. 5) is a bright and fast-rotating star ($v \sin i = 310$ km s^{-1}), and is a member of the Scorpio-Centaurus OB association (de Geus et al. 1989). It rotates at 0.65 of its critical velocity (Hutchings et al. 1979) and the estimated mass-loss rate from Si IV doublet profiles is $\log \dot{M} = -9.55\ M_{\odot}\ {\rm yr}^{-1}$ (Snow 1982). Stefl et al. (1995) found a nearly sinusoidal variation in the radial velocity of Si III 4552 Å with a period of 0.6424 day. In the near-infrared spectrum η Cen presents weak lines of C I and Mg II. Fe II 10 500 Å is symmetrically double-peaked (−175 and 260 km s^{-1}), while Fe II 10 862 Å and Fe II 10 872 Å are blended. He I 10 830 Å displays a shell feature (central intensity of $F/F_{\rm c}$ = 0.4), indicating that this object is seen nearly at the equator. Pa γ shows a complex structure, with three emission peaks.

***δ* Centauri** (Fig. 6) is a member of the Sco-Cen OB association, and Fleming (1890) again was the first to detect its emission-line features. Hanuschik et al. (1995) found V/R variability in Hα and Fe II lines, which he proposed to be due to global disk oscillations. Clark et al. (1998) identified δ Cen as a radio source, which may be variable. In the near-infrared region it shows a rich variety of Fe II lines. Fe II 10 490 Å and Fe II 10 525 Å are weak ($F_{\rm peak}/F_{\rm c} = 1.05$), while Fe II 10 500 Å appears double peaked (−60 and +80 km s^{-1}). The Fe II 10 862 Å profile is double-peaked too (−88 and +30 km s^{-1}). We found weak emission lines at 10 541 Å and 10 550 Å which we identified as N I 10 539.6 Å and 10 549.6 Å, respectively. The blend of C I lines is weak ($F_{\rm peak}/F_{\rm c} = 1.05$), peaking at 10 684 Å and 10 692 Å. The He I 10 830 Å line shows a broad profile, reaching up to $F_{\rm peak}/F_{\rm c} = 1.15$. Pa γ is strong ($F_{\rm peak}/F_{\rm c} = 1.25$) and the peak is slightly redshifted (+25 km s^{-1}). The Mg II lines are present as well.

***α* Arae** (Fig. 5) does not show V/R variability in the optical spectrum, presenting only a constant and moderated Balmer emission (Mennickent 1991; Hanuschik et al. 1995). In our spectrum it presents double-peaked Fe II emission both in 10 500 Å (−105 and +142 km s^{-1}) and 10 862 Å (−60 and +80 km s^{-1}). As almost all Be stars of our atlas, it displays a broad emission at 10 686 Å that we identified as a blend of C I lines (10 683 Å, 10 685 Å and 10 691 Å). An unidentified absorption feature was found at 10 906 Å. α Arae also shows weak emission of Mg II 10 915 Å and 10 952 Å, and very weak ($F_{\rm peak}/F_{\rm c} = 1.05$) emission of He I 10 830 Å. Pa γ is strong and double-peaked (−109 and +85 km s^{-1}).

***λ* Pavonis** (Fig. 7) is a intermediate-rotating Be star ($v \sin i$ = 140 km s^{-1}). This object revealed highly-variable Hβ emission episodes during 1984–1987 (Mennickent 1991). Our monitoring at Observatório Pico dos Dias have shown many episodes of fading and reappearance of Hα during the last 15 yr (Damineli 2007, in preparation). Its optical spectrum shows strong, double-peaked H emission (Sahade et al. 1988). Chen et al. (1989) analyzed its IUE spectra and found that the profiles of the UV lines are rotationally broadened into two groups, with rotational velocities of 170 and 210 km s^{-1}. They inferred two different regions in the extended stellar atmosphere, one that is rotating and one expanding, carrying the wind out at a maximum velocity of 155 km s^{-1}. Only absorption lines are found in the IUE spectra of λ Pav, ranging from neutral species (e.g., C I and N I) to highly ionized ions (C IV and Si IV). This object was detected as a hard X-ray source by the Einstein Observatory and might have a neutron star as a companion. The only line present in its near-infrared spectrum is He I 10 830 Å, with $F_{\rm peak}/F_{\rm c} = 1.45$, and symmetrically double-peaked (−130 and +130 km s^{-1}).

HD 142983 (Fig. 5) is a V/R variable star with an extended atmosphere. It shows cyclical variations with a period of about 10 yr. In the UV spectrum it does not show any emission lines, and the optical H and He lines are broadened by rotation (McLaughlin 1961; Delplace & Chambon 1976). Floquet et al. (1996) showed multiple-frequency patterns in the line-profile variations in HD 142983. They suggested that non-radial pulsations and enhanced mass-loss rates are linked in Be stars. The near-infrared spectrum of HD 142983 shows Fe II 10 500 Å symmetrically double-peaked (−135 and +127 km s^{-1}) and Fe II 10 862 Å double-peaked too, but non-symmetrically (−150 and +95 km s^{-1}). C I and Mg II lines are present, but very weakly. He I 10 830 Å shows a shell-like absorption profile ($F/F_{\rm c} = 0.3$), indicating that HD 142983 is seen nearly equator-on. The same unidentified feature found in α Arae at 10 906 Å was found here as well. Pa γ shows a shell profile, consisting of two emission shoulders separated by a strong absorption feature, centered at −40 km s^{-1}.

***β* Monocerotis A** (Fig. 7) is the brightest member of a complex triple system where the three components are Be stars of similar spectral type (Maranon di Leo et al. 1994). β Mon A shows V/R variability with a period of 12.5 yr (McLaughlin 1961). Mara et al. (1991) reported profile variation of Mg II 4481 Å, showing episodic emissions. Its near-infrared spectrum resembles HD 142983, except for some unidentified features in the former. It shows Fe II 10 500 Å double-peaked (−48 and +190 km s^{-1}) as well as Fe II 10 862 Å (−80 and +135 km s^{-1}). Fe II 10 525 Å is also clearly present. We detected a broad emission around 10 689 Å which we identified as a blend of C I (10 683, 10 685, 10 691 Å). We also detected narrow emissions at 10 714, 10 723 Å, which we related to a double-peaked emission of N I 10 718 Å (−70 and +150 km s^{-1}, respectively). We found a broad emission at 10 740 Å and very narrow absorptions at 10 757 Å and 10 770 Å that remain unidentified. He I 10 830 Å displays a shell absorption ($F/F_{\rm c}$ = 0.65), indicating that this object is seen nearly equator-on. Pa γ is double-peaked (−70 and +110 km s^{-1}), presenting a strong absorption centered at 30 km s^{-1}. The line intensity drops from $F/F_{\rm c}$ = 2.0 in the Doppler-shifted peaks to $F/F_{\rm c}$ = 1.4 in the dip.

3.2. O, B, and A Iape Stars – or LBVs, LBV candidates and dormant LBVs

The spectra of OBA Iape stars are presented in Figs. 8–11. We grouped peculiar objects that share common morphological properties in the same figure, although this is almost impossible in some cases. The stars in this group are all related to the LBV phase; some of them are known as bona fide LBVs (such as AG Car and HR Car), some are LBV candidates (W 243 in Westerlund 1, MWC 314) and some are believed to be in a dormant/post-LBV phase (such as He 3-519). For a recent review on the properties of these objects see Humphreys & Davidson (1994), van Genderen (2001), and Clark et al. (2005).

HD 168625 (Fig. 8) is classified as a marginally-dormant LBV based on its last 25-year lightcurve (Sterken et al. 1999), although a typical LBV nebula was discovered around it (Hutsemekers et al. 1994; Nota et al. 1996; Robberto & Herbst 1998; Pasquali et al. 2002; O'Hara et al. 2003). Its optical

spectrum was recently published by Chentsov et al. (2003), while Hanson et al. (1996) showed the *K*-band spectrum. Our spectrum shows weak emission lines of Fe II, Mg II and NI. He I 10 830 Å shows a deep P Cyg absorption with a very weak emission, while Pa γ is seen in absorption. As in HR Car, we also detected the 10 780 Å and the 10 792 Å absorption features. The comparison between the 2001 and 2004 datasets do not show any evidence of variations in the spectral lines, confirming its current dormant stage.

HD 168607 (Fig. 8) is only 62″ away from HD 168625 in the sky, and they are both believed to be members of the M 17 association, lying at 2.2 kpc (WF2000). At this distance they would be separated by only 0.7 pc in projection, and regarding their similar blue spectra, it has been proposed that they could be a pair of massive twin stars (see discussion in WF2000). The 25-year lightcurve of HD 168607 presented by Sterken et al. (1999) shows the same qualitative behavior of other LBVs, such as AG Car, but on a much longer timescale. In our atlas, the near-infrared spectrum of HD 168607 resembles that of HD 168625, although the former shows more developed emission lines, suggesting a higher activity and a higher mass-loss rate for HD 168607. This objected has also shown spectroscopic variations in the last 3 yr (Fig. 18), with an increase in the absorption of He I 10 830 Å and an overall decrease in the intensity of the emission lines.

HD 160529 (Fig. 8) is a bright A-type hypergiant star. Sterken et al. (1991), through Strömgren *uvby* and near-infrared photometry, found a change in the spectral type from A9 to B8 between 1983 and 1991, and a brightness decrease of 0.5 mag in this period. Based on this behavior, they classified HD 160529 as an LBV star, and analyzed its lightcurve variations as well. Its spectral variability was analyzed by Wolf et al. (1974), who found variations in the Balmer lines profile and in the radial velocities of about 40 km s^{-1}. More recently Stahl et al. (2003) reported a long-term spectroscopic monitoring and the recent lightcurve of HD 160529. They found little variation in the spectral type around A2Ia from 1991 to 2002, mainly using He I 5876 Å as a diagnostic line. In our atlas, the near-infrared spectrum of HD 160529 is very similar to the spectrum of HR Car, except that the former shows stronger emission in He I 10 830 Å, with a P Cyg profile. Moreover, Pa γ is seen in absorption. From 2001 to 2004 we detected a radial velocity variation of 55 km s^{-1}. We also noticed an overall increase in the strength of the absorption lines, with a new absorption feature appearing at 10 581 Å, and a drastic decrease in the Fe II emission. However, He I 10 830 Å did not change its strength (Fig. 18).

HR Carinae (Fig. 8) is one of the rare bona-fide LBV stars in the Galaxy. Its variability was first reported by Hertzsprung (Hoffleit 1940), and since then several lightcurves have been published (see van Genderen et al. 1997). The high values of the luminosity and mass-loss rate of HR Car were first noted by Viotti (1971), and the 1989–1990 spectral variability with the associated changes in the lightcurve were analyzed by Hutsemekers & van Drom (1991). Their optical spectra show evidence of an expanding atmosphere with multiple shells. The spectrum of the bipolar nebula associated with HR Car shows evidence of nitrogen enrichment, as does the star itself. A detailed study of the optical nebula around HR Car is given in Nota et al. (1997) and Weis et al. (1997), and the mid-infrared imaging of the nebula is presented by Voors et al. (1997). The most recent analysis of the wind of HR Car was performed by Machado et al. (2002), based on spectra collected in April 1999. They derived an effective temperature of 10 000 K, a luminosity of 500 000 $L_\odot$ and a mass-loss rate of 6.5×10^{-5} $M_\odot$ yr^{-1}. Previously, van Genderen (2001) derived an effective temperature of 8000 K for HR Car in 1992, while Nota et al. (1997) found 20 000 K (May 1995) and 15 000 K (January 1996). The near-infrared spectra of HR Car in June 2001 shows weak Fe II emission (10 500 Å, 10 525 Å 10 862 Å and 10 871 Å). Pa γ shows an inverse P Cygni profile, while He I 10 830 Å is almost absent, with a very weak broad emission. HR Car shows a rich absorption spectrum of N I, C I and Mg II. An unidentified feature was found at 10 780 Å and another at 10 792 Å (see Sect. 4). The data taken in 2004 show much more variability than in 2001 (Fig. 18). The inverse P Cyg profile of Pa γ changed to a pure strong emission, with the equivalent width rising from 2 to 14 Å. The Fe II lines became stronger too, while the Mg II lines that were present in absorption turned into emission. The line of He I 10 830 Å presented an intrincated profile, with a double-peak emission superimposed on the previous broad emission.

W 243 (Fig. 8) is a recently-discovered LBV candidate in the massive, young open cluster Westerlund 1 (Clark & Negueruela 2004). Those authors presented an optical spectrum characterized by a double-peaked emission of Hα and single-peaked emission in the He I lines. They also reported the strengthening of Hα during 2001–2003. The comparison with older spectra revealed that the star evolved from B2-5Ia to A2I from 1981 to 2003, suggesting an LBV classification. A *K*-band spectrum obtained by Groh et al. (2006a) in July 2005 suggests further evolution towards a hotter temperature. In this work we obtained near-infrared data in 2004 that confirm its LBV nature. Its spectrum is similar to other cool LBVs, showing a strong Pa γ emission that resembles HR Car as it was in 2004. Another remarkable feature of cool LBVs, namely, the presence of Mg II, N I and C I lines in absorption, are also seen in W243. However, He I 10 830 Å emission is present and stronger than in other cool LBVs. The P-Cygni absorption of this line is noticeable, extending up to 400 km s^{-1}, which is much higher than the expected wind terminal velocity for A supergiants. Further monitoring of W 243 is required to address the origin of this high-velocity absorption.

***η* Carinae** (Fig. 9) is one of the most observed stars. It underwent a giant eruption in the 1840 s that generated the bipolar-shaped *Homunculus* nebula (Gaviola 1950), and another outburst in the 1890 s that probably generated another nebula, the "little Homunculus" (Ishibashi et al. 2003). The reader is referred to Davidson & Humphreys (1997), who reviewed the system and its environment. Since then, many works related to the nature of the central source in η Car have been published, mainly regarding the 5.54-year cycle and the binary scenario (Damineli et al. 1997) or alternative ones (Davidson 1997). Its near-infrared spectrum shows prominent Fe II emission at 10 500 Å, 10 525 Å, and 10 862 Å, with a broad and a narrow component. Pa γ also shows the same shape of the Fe II lines. He I 10 830 Å is stronger, with a P Cygni profile extending up to −660 km s^{-1}. There are other absorptions at −380, −195 and −45 km s^{-1}. The changes in this spectral region are dramatic over the 5.54-year cycle (Fig. 17): a few days before 2003.5 (minimum of the spectroscopic event, see Steiner & Damineli 2004) the narrow emission components from Fe II, He I and Pa γ shrunk until they faded completely. The behavior of He I 10 830 Å is striking: the emission components faded almost completely, while the absorption component of the P Cyg profile extended up to −1300 km s^{-1}.

He 3-519 (Fig. 9) is a galactic prototype of the WN11h class. Its optical and ultraviolet spectrum is nearly identical to

the well-known LBV AG Carinae at minimum (i.e., during the hot phase), as discussed by Smith et al. (1994) and WF2000. Although He 3-519 does not have the typical photometric or spectroscopic behavior of a LBV, it shows a circumstellar nebula that relates it to that class. Therefore, it is believed that He 3-519 belongs to a rare class of post-LBV, pre-WN stars (Davidson et al. 1993). The near-infrared spectrum of He 3-519 is similar to that of HD 316285, but the former displays a stronger He I 10 830 Å emission and is almost free of Fe II lines. The 2001−2004 data evolution shows significant strengthening of He I 10 830 Å, but without changes in the velocity of the edge of the P Cyg absorption (Fig. 17), resembling the pattern of the variations of HD 316285.

HD 316285 (Fig. 9) is a luminous, evolved massive star as discussed in Hillier et al. (1998). Based on a detailed spectral analysis, those authors found evidence for nitrogen and helium enhancement on the stellar surface, and a large mass-loss rate of $2.4 \times 10^{-4}\ M_{\odot}\,\mathrm{yr}^{-1}$ was derived. Although there is no evidence of photometric variability, Hillier et al. also noticed spectroscopic variation, specially in the Fe II lines. The near-infrared spectrum of this star resembles that of η Car, except that the nebular and high-excitation lines seen in the former are not present in HD 316285. Also, He I 10 830 Å does not show the additional absorption components seen in the spectrum of η Car. Regarding the variability of HD 316285, our 3 datasets from 2001 to 2004 show significant strengthening of the emission lines (Fig. 17), although no variations are noticed in the velocity of the wind (as seen from the P-Cyg absorption).

MWC 314 (Fig. 10) is a scarcely-studied emission line star. It was first identified by Merrill (1927), while Allen (1973) reported a late-type spectral energy distribution for this object. It was recognized as a high-luminosity B[e] star by Miroshnichenko (1996), who estimated its stellar parameters ($\log L/L_{\odot} = 6.2$, $T = 30\,000$ K, $M = 80\ M_{\odot}$) and derived a high reddening ($A_V = 5.7$ mag). A comparison between B[e] supergiants and LBVs led him to propose that MWC 314 is an LBV candidate. A high resolution optical spectrum of this star is presented by Miroshnichenko et al. (1998); its optical spectrum is dominated by emissions of H I, He I and Fe II. Its near-infrared spectrum resembles AG Car and P Cygni. However, its spectroscopic evolution shows an intriguing behavior in He I 10 830 Å, with a variable high-velocity absorption wing extending up to 1500 km s^{-1} (Fig. 18). This behavior is striking because such a high velocity is not expected for this kind of object. In Fig. 5 of Miroshnichenko et al. (1998) a high-velocity absorption can be seen in He I 5876 Å, although errors in the continuum normalization may affect the interpretation (Miroshnichenko, private communication). Moreover, the same qualitative behavior appears in η Car during periastron passage, although much more dramatically in the latter (see Fig. 17). Additional multi-wavelenght observations of MWC 314 using a finer temporal sampling are required to address the origin of this high-velocity absorption component. The equivalent width of the emission lines also changed by a factor of 1.5 from 2001 to 2004.

AG Carinae (Fig. 10) is the "Rosetta Stone" of the LBV class, lying at 6 kpc from the Sun (Humphreys et al. 1989). AG Car and its environment have been extensively studied in the last decades. The star is surrounded by a bipolar nebula first reported by Thackeray (1950), which was ejected from the star $\sim 10^4$ yr ago (Nota et al. 1992; de Freitas Pacheco et al. 1992; Lamers et al. 2001). The photometric variability in the last century was analyzed by van Genderen et al. (1997), while the recent spectroscopic variability was studied by Leitherer et al. (1994) and Stahl et al. (2001). The morphology and kinematics of the ejecta were analyzed by Nota et al. (1995), and the nebular abundances were determined by Smith et al. (1997). Shore et al. (1996) found a color excess of $E(B-V) = 0.65$ for AG Car based on IUE data. The optical spectra at minimum were analyzed by Smith et al. (1994), who found an enhanced helium abundance at the surface of the star. Recently, Groh et al. (2006b) found that AG Car is rotating very fast (up to 0.86 of its critical velocity), and therefore it lies close to the so-called $\Gamma\Omega$ limit (Maeder & Meynet 2000a). The AG Car near-infrared spectrum shows prominent emission lines of Fe II and Mg II, and weak emission of C I and N I. He I 10 667 and 10 830 Å show P Cygni profiles and Pa γ is seen in emission. The variability of the lines from 2001 (hot phase) to 2004 (cool phase) is striking in this spectral region, specially in He I 10 830 Å (Fig. 18). The line equivalent width dropped from 122 Å in 2001 to 0.2 Å in 2004. Also, in 2001 an additional absorption component appeared in this line.

P Cygni (Fig. 10) is a famous member of the LBV class, sharing its name to denote the characteristic shape of the spectral lines present in those stars. P Cyg underwent a major eruption in the 1600 s, lying in a quiescent phase since then. This eruption (and perhaps a previous one) gave rise to complex ejecta around the star (Skinner et al. 1998; Chesneau et al. 2000; Exter et al. 2002). The atmospheric parameters derived by Najarro et al. (1997) revealed a helium-enriched photosphere and confirmed the high mass-loss rate and luminosity of the star. A conference regarding the latest P Cyg progresses was organized in 2000; we refer the reader to the proceedings of the event (ASP Conf. Proceedings 233) for a general review. The near-infrared spectrum of P Cygni is very similar to AG Car at minimum. It shows strong He I 10 830 Å and Pa γ emission, followed by more modest Fe II and Mg II emission. From 2001 to 2003 the emission lines of P Cyg became stronger, and since then they started to fade (Fig. 18).

HD 326823 (Fig. 11) is located in the direction of the Galactic Center at a distance of 2 kpc (McGregor et al. 1988). Sterken et al. (1995) suggested that HD 326823 could be a LBV in a quiescent state, based on their photometric study. (Lopes et al. 1992) presented the optical and the 1 μm spectrum of this object. The majority of the lines are double-peaked, probably indicating deviations from spherical symmetry and suggesting the presence of a disk. The helium and nitrogen lines are the strongest ones, while Hα and Hβ are weakly present. Hence, they concluded that HD 326823 is an evolved star, entering the Wolf-Rayet phase. Borges Fernandes et al. (2001) present a high-resolution optical atlas of this star, identifying the strongest features. The lines in the near-infrared spectrum show the same double-peaked morphology as the optical ones. The strongest emission line seen is He I 10 830 Å, followed by Fe II and Mg II lines. Pa γ and C I lines are barely seen. Unfortunately, we observed HD 326823 only in the 2001 run, preventing us from studying the variability of the star.

GG Carinae (Fig. 11) is suggested to be an eclipsing binary with a period of 31 or 62 days (Hernandez et al. 1981; Gosset et al. 1985), although the radial velocity curve is not well determined. The ultraviolet spectrum was published by Brandi et al. (1987), who recognize numerous Fe II and Ni II features. Our near infrared data from 2001 shows Fe II, Mg II, C I and He I 10 830 Å in emission. Pa γ is the strongest line in our spectrum, showing a blueshifted feature at 10 931.5 Å, that we could not identify, which may be a component of Pa γ formed in a high-velocity shell.

HD 87643 (Fig. 11) is thought to be an evolved B[e] star (Oudmaijer et al. 1998) and appears to be related to the LBV class, although the link is not clear yet. This object has an optical spectrum dominated by emission lines of Fe II and P Cygni profiles in the Balmer series, together with low excitation forbidden lines. The spectrum is produced by a fast polar wind combined with a slow disk wind (Oudmaijer et al. 1998). The ultraviolet and optical spectra of HD 87643 was previously discussed by de Freitas Pacheco et al. (1982, 1985), who reported a strong spectral line variability. HD 87643 has a bright reflection nebula, which was analyzed by Surdej et al. (1981) and Surdej & Swings (1983). Its 2001 near infrared spectrum shows prominent Fe II, CI lines and Pa γ emission, compatible with the presence of a cold wind. He I 10 830 Å presents a P-Cygni profile, with a weak emission and a strong absorption that goes up to -1750 km s^{-1}, which is probably formed in the fast polar wind.

3.3. OB supergiants

In Fig. 12 we present the OB supergiants of our sample, some of them which are related to the LBV class. The stars are presented in decreasing order of spectral type. The spectra of the OB supergiants typically show He I 10 830 Å with a P Cyg profile and He I 10 667 Å, He I 10 913 Å and Pa γ in absorption, with a variable veiling of their absorption depending on how developed the wind is, culminating with HD 152408, that has only emission lines. The later subtypes also present weak emission of Fe II 10 862 Å, Mg II 10 915 Å and Mg II 10 952 Å.

HD 152408 and **HD 151804** (Fig. 12) are closely-associated O supergiants in Sco OB1. The stellar wind of HD 152408 is stronger despite the fact that the evolutionary difference between both stars must be very small (see WF2000). Both objects were analyzed by Crowther & Bohannan (1997) who derived similar stellar parameters but a higher mass-loss rate and a higher helium content in HD 152408 than in HD 151804, indicating the more evolved nature of the former. The morphology of their near-infrared spectra agrees with the analysis of Crowther & Bohannan (1997), with HD 152408 having strong emission of He I 10 830 Å, He I 10913 Å and Pa γ, while HD 151804 shows the same morphology as the hotter B supergiants stars. An unidentified feature is seen at 10 922.5 Å in emission in HD 152408, while in HD 151804 it is in absorption.

HD 154090 (Fig. 12) is thought to be a normal B supergiant star, with an abundance typical of early-type stars (Kane et al. 1981). Indeed, the near-infrared spectrum that we present is similar to other B supergiants. However, there are significant variations between the 2001 and the 2004 datasets, especially in He I 10 830 Å (Fig. 18). In three years, the equivalent width of this line reduced by a factor of two, with the P Cyg absorption almost disappearing. These changes occurred together with radial velocity variations of $\sim$120 km s^{-1}, and minor changes in the absorption profiles of Pa γ and He I 10 913 Å. This behavior encourages future monitoring of this star for better insight into its nature.

HD 169454 (Fig. 12) is a member of the Sct OB3 association, located at 1.5 kpc from the Sun (Humphreys 1978). However, the analysis of the high-velocity interstellar gas in the direction of HD 169454 puts the star at least at 3 kpc, which yields an absolute magnitude of $M_V \sim -9.2$. As a consequence, HD 169454 may be one of the brightest B-type stars in the Galaxy. Its optical spectrum was analyzed by Rivinius et al. (1997), who found a variability pattern similar to that shown by HD 152236. We found that their near-infrared spectrum and the changes from 2001 to 2004 are very similar as well (Fig. 16).

HD 152236 (Fig. 12) is located in the Sco OB1 association, belonging to the open cluster NGC 6231 (van Genderen et al. 1984). Photometric variability in this object was reported by Sterken (1977) and Sterken et al. (1997), who suggested the relationship between the cyclic charactheristics of the lightcurve of HD 152236 and the LBV class. These authors also claim an increase in the apparent visual magnitude through the past centuries, with the star being 2 mag brighter in the 18th century. Burki et al. (1982) analyzed the UV variability, showing the presence of discrete absorption components (DACs). Rivinius et al. (1997) investigated the changes in the optical spectrum revealing an intense variability during 1990–91. The quantitative study of the spectrum by these authors also confirm that HD 152236 is a very luminous star ($\log L/L_\odot = 6.05$). Its near-infrared spectrum shows He I 10 830 Å with a P Cyg profile with an absorption extending up to -450 km s^{-1} and He I 10 667 Å, He I 10 913 Å and Pa γ in absorption. The comparison between spectra taken in 2001 and 2004 shows radial velocity changes of about 120 km s^{-1} and in the profile of He I 10 830 Å. Also, the emission was stronger and the absorption was shallower in 2001 when compared to the 2004 dataset (Fig. 16).

HD 80077 (Fig. 12) is a very luminous B star ($M_{\rm Bol} = -11$) with a comparatively low mass-loss rate of 5×10^{-6} $M_\odot$ yr^{-1} (Carpay et al. 1989, 1991) among luminous B stars. These authors claim that the star could be an LBV, since it has a low surface gravity and a high luminosity. Historical observations also suggest that the mass-loss rate was higher some decades ago (Houk 1978). The lightcurve presented by van Genderen et al. (1992) shows that during 15 yr the star had an apparent visual magnitude of $m_V = 7.5$, with micro-variations of about 0.05 mag. It is still not known why HD 80077 is such a stable star, while its LBV neighbors in the HR diagram are unstable. We observed this star only in 2001, and its near-infrared spectrum is very similar to other luminous B stars, such as HD 152236 and HD 169454. The only noticeable difference is the partial filling of the Pa γ absorption and the presence of Mg II lines in emission. HD 80077 also displays an unidentified absorption feature at 10 700 Å.

3.4. Wolf-Rayet stars

We have obtained spectra of 4 WN stars (Fig. 13) and 3 WC stars (Fig. 14). All of them are listed in the VIIth Catalog of Galactic Wolf-Rayet stars (van der Hucht 2001), where their properties are extensively listed. Physical properties of WR stars are thoroughly reviewed in Crowther (2007).

The spectra of the WN stars, namely **WR 6** (WN4), **WR 136** (WN6(h)), **WR 78** (WN7h) and **WR 22** (WN7h+O9III-V), show a very strong P Cygni profile in He I 10 830 Å blended with emission in Pa γ. The WNE stars WR 6 and WR 136 show flat-topped line emission profiles, while the later WN stars of our sample show a more round-topped line emission profile. In WR 22 it is also noticeable the He I 10 830 Å absorption from the O9 star.

Our sample of WC stars contains only the later subtypes (**WR 90** = WC7, **WR 11** = WC8+O and **WR 103** = WC9d). This class of objects shows a broad, strong emission of He I 10 830 Å with a small P Cyg absorption. There is also a blended emission from C III + C IV centered at 10 545 Å. In the WC9d star WR103 there is an emission of He I 10 913 Å that indicates its cool nature compared to other WC stars. In WR 11 (γ^2 Vel) the Pa γ absorption from the secondary star (O7.5III-V) is also prominent.

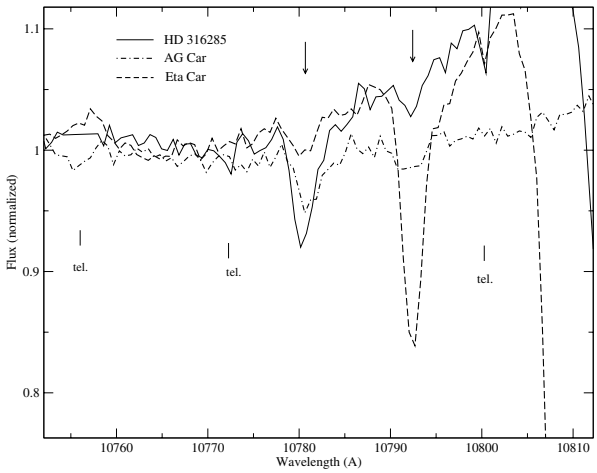

Fig. 2. Unidentified absorption lines found in the LBVs HD 316285 (full), AG Car (dot-dashed) and η Car (dashed) at 10 780 Å and at 10 792 Å (arrows). The position of the strongest telluric lines are also indicated, to show that they do not contaminate the absorption features.

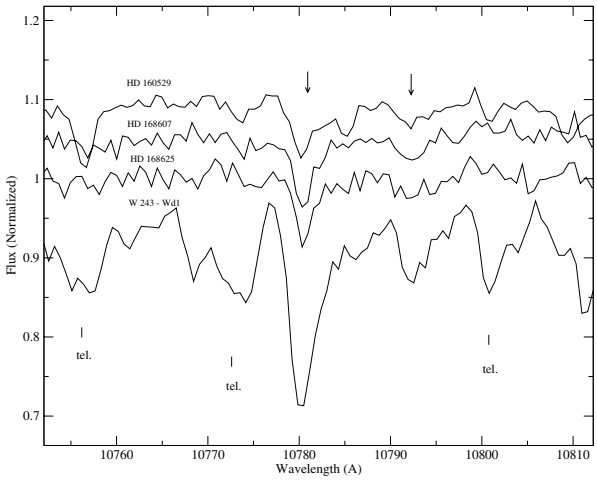

Fig. 3. Same as Fig. 2, showing the presence of the same absorption lines in HD 160529, HD 168607, HD 168625 and W243. For clarity, the spectra were shifted up by an arbitrary offset.

4. Discussion: unidentified absorption features

In the previous section we presented unambiguous identification of most emission lines present in the spectral region covered by this work. The presence of C I lines in Be stars and LBVs is remarkable, as carbon is expected to be depleted in those objects, either due to rotational mixing or by the ejection of the outer layers. The near-infrared C I lines potentially can be used to constrain the carbon abundance in these stars.

However, the presence of unidentified absorption features is striking in most of the LBVs at 10 780 Å and 10 792 Å, some of which do not have any photospheric absorption lines in their spectra (e.g. η Car). Figures 2 and 3 display a zoom around those absorption lines. Their similar strength in stars spanning a range of spectral types, together with their constance in variable stars such as LBVs, make it likely that the unidentified absorption features arise in the interstellar or circumstellar medium of those stars. The comparison between the EW of the absorption line found at 10 780 Å and the color excess $E(B-V)$ is displayed in Fig. 4. A correlation is clearly seen between these quantities,

$$E(B-V) \simeq 0.16(0.14) + 6.19(0.53) \times EW_{10780}. \quad (1)$$

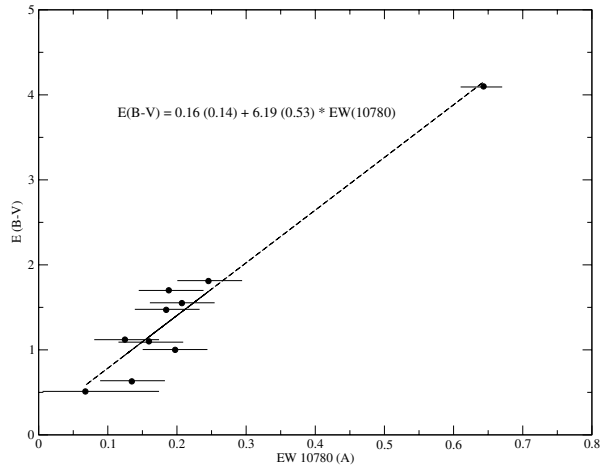

Fig. 4. Calibration of EW (10 780) versus $E(B-V)$. The color excesses $E(B-V)$ were taken from van Genderen (2001), except for W243 (Teodoro, private communication). A least-squares linear fit to the data is also shown (see Eq. (1)).

Such a tight correlation can be used to constrain circumstellar properties of LBVs. Additional observations with higher resolution and *S/N* are underway, and will be discussed in a forthcoming paper.

Compared to the feature at 10 780 Å, the absorption at 10 792 Å is weaker in all objects except η Car. Hence, it is difficult to perform a similar calibration as the one made for the 10 780 Å feature. An observing campaign is underway by our group to address this point. Nevertheless, this line is much stronger in Eta Car than in other stars with similar interstellar reddening. It was previously interpreted as a high-velocity (-1040 km s^{-1}) component of the stellar He I 10 830 Å (Damineli et al. 1993; Smith 2002). However, this line is present in several other LBVs which do not present any high-velocity component, and it is constant in η Car along its spectroscopic event. Therefore, we suggest that it is formed in the circumstellar environment of η Car. Indeed, if true, a precise calibration between EW(10 792 Å) and $E(B-V)$ may indicate the amount of circumstellar reddening present in η Car, which is still speculative. It would also provide constraints on the luminosity and nature of η Car and other objects with unknown amounts of circumstellar reddening.

Acknowledgements. We are grateful to the referee Dr. J. Puls for construtive suggestions and detailed comments. J.H. Groh and A. Damineli thank Brazilian Agencies FAPESP (grants 02/11446-5 and 2005/51742-0) and CNPq (grant 200984/2004-7) for financial support. J.H. Groh acknowledges suppport from CNPq through its undergraduate research program (PIBIC). This work made extensive use of the SIMBAD database, which is operated by CDS. We thank Dr. Peter van Hoof for making available his atomic line database.

References

Allen, D. A. 1973, MNRAS, 161, 145
Andrillat, Y., & Vreux, J. M. 1979, A&A, 76, 221
Banerjee, D. P. K., Janardhan, P., & Ashok, N. M. 2001, A&A, 380, L13
Barker, P. K., & Marlborough, J. M. 1985, ApJ, 288, 329
Borges Fernandes, M., de Araújo, F. X., Bastos Pereira, C., & Codina Landaberry, S. J. 2001, ApJS, 136, 747
Borisova, I. K. 1992, Ap&SS, 195, 303
Brandi, E., Gosset, E., & Swings, J.-P. 1987, A&A, 175, 151
Burki, G., Heck, A., Cassatella, A., & Bianchi, L. 1982, A&A, 107, 205
Carpay, J., de Jager, C., Nieuwenhuijzen, H., & Moffat, A. 1989, A&A, 216, 143
Carpay, J., de Jager, C., & Nieuwenhuijzen, H. 1991, A&A, 248, 475
Chen, H., Ringuelet, A., Sahade, J., & Kondo, Y. 1989, ApJ, 347, 1082

Chentsov, E. L., Ermakov, S. V., Klochkova, V. G., et al. 2003, A&A, 397, 1035
Chesneau, O., Roche, M., Boccaletti, A., et al. 2000, A&AS, 144, 523
Clark, J. S., & Negueruela, I. 2004, A&A, 413, L15
Clark, J. S., Steele, I. A., & Fender, R. P. 1998, MNRAS, 299, 1119
Clark, J. S., Tarasov, A. E., Okazaki, A. T., Roche, P., & Lyuty, V. M. 2001, A&A, 380, 615
Clark, J. S., Larionov, V. M., & Arkharov, A. 2005, A&A, 435, 239
Codina, S. J., de Freitas Pacheco, J. A., Lopes, D. F., & Gilra, D. 1984, A&AS, 57, 239
Crowther, P. A. 2007, ARA&A, in press
Crowther, P. A., & Bohannan, B. 1997, A&A, 317, 532
Crowther, P. A., Lennon, D. J., & Walborn, N. R. 2006, A&A, 446, 279
Dachs, J., & Hanuschik, R. 1984, A&A, 138, 140
Damineli, A., Viotti, R., Baratta, G. B., & de Araujo, F. X. 1993, A&A, 268, 183
Damineli, A., Conti, P. S., & Lopes, D. F. 1997, New Astron., 2, 107
Davidson, K. 1997, New Astron., 2, 387
Davidson, K., & Humphreys, R. M. 1997, ARA&A, 35, 1
Davidson, K., Humphreys, R. M., Hajian, A., & Terzian, Y. 1993, ApJ, 411, 336
de Freitas Pacheco, J. A., Gilra, D. P., & Pottasch, S. R. 1982, A&A, 108, 111
de Freitas Pacheco, J. A., Faria Lopes, D., Landaberry, S. C., & Selvelli, P. L. 1985, A&A, 152, 101
de Freitas Pacheco, J. A., Damineli Neto, A., Costa, R. D. D., & Viotti, R. 1992, A&A, 266, 360
de Geus, E. J., de Zeeuw, P. T., & Lub, J. 1989, A&A, 216, 44
Delgado-Martí, H., Levine, A. M., Pfahl, E., & Rappaport, S. A. 2001, ApJ, 546, 455
Delplace, A. M., & Chambon, M. T. 1976, in Be and Shell Stars, IAU Symp., 70, 79
Doazan, V. 1970, A&A, 8, 148
Exter, K. M., Watson, S. K., Barlow, M. J., & Davis, R. J. 2002, MNRAS, 333, 715
Fabregat, J., Reig, P., & Otero, S. 2000, IAU Circ., 7461, 1
Fabregat, J., Reig, P., & Tarasov, A. 2002, Be Star Newsletter, 35, 10
Fleming, W. P. 1890, Astron. Nachr., 123, 383
Floquet, M., Hubert, A. M., Hubert, H., et al. 1996, A&A, 310, 849
Gaviola, E. 1950, ApJ, 111, 408
Gosset, E., Hutsemekers, D., Swings, J. P., & Surdej, J. 1985, A&A, 153, 71
Grady, C. A., Sonneborn, G., Wu, C.-C., & Henrichs, H. F. 1987, ApJS, 65, 673
Gräfener, G., Koesterke, L., & Hamann, W.-R. 2002, A&A, 387, 244
Grigsby, J. A., Morrison, N. D., & Anderson, L. S. 1992, ApJS, 78, 205
Groh, J. H., Damineli, A., Teodoro, M., & Barbosa, C. L. 2006a, A&A, 457, 591
Groh, J. H., Hillier, D. J., & Damineli, A. 2006b, ApJ, 638, L33
Hamann, W.-R., & Koesterke, L. 1998, A&A, 335, 1003
Hanson, M. M., Conti, P. S., & Rieke, M. J. 1996, ApJS, 107, 281
Hanuschik, R. W., & Vrancken, M. 1996, A&A, 312, L17
Hanuschik, R. W., Hummel, W., Dietle, O., & Sutorius, E. 1995, A&A, 300, 163
Heasley, J. N., & Wolff, S. C. 1983, ApJ, 269, 634
Hernandez, C. A., Sahade, J., Lopez, L., & Thackeray, A. D. 1981, PASP, 93, 747
Hillier, D. J., Crowther, P. A., Najarro, F., & Fullerton, A. W. 1998, A&A, 340, 483
Hillier, D. J., Davidson, K., Ishibashi, K., & Gull, T. 2001, ApJ, 553, 837
Hillier, D. J., & Miller, D. L. 1998, ApJ, 496, 407
Hoffleit, D. 1940, Harvard College Observatory Bulletin, 913, 4
Houk, N. 1978, Michigan Catologue of Spectral Types 2
Hubeny, I., & Lanz, T. 1995, ApJ, 439, 875
Hubeny, I., Harmanec, P., & Stefl, S. 1986, Bull. Astron. Inst. Czech., 37, 370
Humphreys, R. M. 1978, ApJS, 38, 309
Humphreys, R. M., & Davidson, K. 1994, PASP, 106, 1025
Humphreys, R. M., Lamers, H. J. G. L. M., Hoekzema, N., & Cassatella, A. 1989, A&A, 218, L17
Hutchings, J. B., Nemec, J. M., & Cassidy, J. 1979, PASP, 91, 313
Hutsemekers, D., & van Drom, E. 1991, A&A, 248, 141
Hutsemekers, D., van Drom, E., Gosset, E., & Melnick, J. 1994, A&A, 290, 906
Ishibashi, K., Gull, T. R., Davidson, K., et al. 2003, AJ, 125, 3222
Kane, L. G., McKeith, C. D., & Dufton, P. L. 1981, MNRAS, 194, 537
Lamers, H. J. G. L. M., Nota, A., Panagia, N., Smith, L. J., & Langer, N. 2001, ApJ, 551, 764
Leitherer, C., Allen, R., Altner, B., et al. 1994, ApJ, 428, 292
Levenhagen, R. S., & Leister, N. V. 2006, MNRAS, 371, 252
Lopes, D. F., Damineli Neto, A., & de Freitas Pacheco, J. A. 1992, A&A, 261, 482
Lyubimkov, L. S., Rostopchin, S. I., Roche, P., & Tarasov, A. E. 1997, MNRAS, 286, 549
Machado, M. A. D., de Araújo, F. X., Pereira, C. B., & Fernandes, M. B. 2002, A&A, 387, 151
Maeder, A., & Meynet, G. 2000a, A&A, 361, 159
Maeder, A., & Meynet, G. 2000b, ARA&A, 38, 143
Mara, C., di Leo, N., & Ringuelet, A. E. 1991, Rev. Mex. Astron. Astrofis., 22, 306
Maranon di Leo, C., Colombo, E., & Ringuelet, A. E. 1994, A&A, 286, 160
McGregor, P. J., Hyland, A. R., & Hillier, D. J. 1988, ApJ, 324, 1071
McLaughlin, D. B. 1961, AJ, 66, 48
Meisel, D. D., Frank, Z. A., Packard, M. L., & Saunders, B. A. 1982, ApJ, 263, 759
Mennickent, R. E. 1991, A&AS, 88, 1
Merrill, P. W. 1927, ApJ, 65, 286
Miroshnichenko, A. S. 1996, A&A, 312, 941
Miroshnichenko, A. S., Fremat, Y., Houziaux, L., et al. 1998, A&AS, 131, 469
Miroshnichenko, A. S., Fabregat, J., Bjorkman, K. S., et al. 2001, A&A, 377, 485
Morris, P. W., Eenens, P. R. J., Hanson, M. M., Conti, P. S., & Blum, R. D. 1996, ApJ, 470, 597
Najarro, F., Hillier, D. J., & Stahl, O. 1997, A&A, 326, 1117
Neiner, C., Floquet, M., Hubert, A. M., et al. 2005, A&A, 437, 257
Nota, A., Leitherer, C., Clampin, M., Greenfield, P., & Golimowski, D. A. 1992, ApJ, 398, 621
Nota, A., Livio, M., Clampin, M., & Schulte-Ladbeck, R. 1995, ApJ, 448, 788
Nota, A., Pasquali, A., Clampin, M., et al. 1996, ApJ, 473, 946
Nota, A., Smith, L., Pasquali, A., Clampin, M., & Stroud, M. 1997, ApJ, 486, 338
O'Hara, T. B., Meixner, M., Speck, A. K., Ueta, T., & Bobrowsky, M. 2003, ApJ, 598, 1255
Oudmaijer, R. D., Proga, D., Drew, J. E., & de Winter, D. 1998, MNRAS, 300, 170
Pasquali, A., Nota, A., Smith, L. J., et al. 2002, AJ, 124, 1625
Pauldrach, A. W. A., Hoffmann, T. L., & Lennon, M. 2001, A&A, 375, 161
Peters, G. J. 1982, ApJ, 253, L33
Prinja, R. K., & Henrichs, H. F. 1987, in IAU Colloq. 92: Physics of Be Stars, 265
Puls, J., Urbaneja, M. A., Venero, R., et al. 2005, A&A, 435, 669
Rachford, B. L., Snow, T. P., Tumlinson, J., et al. 2001, ApJ, 555, 839
Rivinius, T., Stahl, O., Wolf, B., et al. 1997, A&A, 318, 819
Robberto, M., & Herbst, T. M. 1998, ApJ, 498, 400
Roche, P., Larionov, V., Tarasov, A. E., et al. 1997, A&A, 322, 139
Sahade, J., Rovira, M., Ringuelet, A. E., Kondo, Y., & Cidale, L. 1988, ApJ, 327, 335
Shore, S. N., Altner, B., & Waxin, I. 1996, AJ, 112, 2744
Skinner, C. J., Becker, R. H., White, R. L., et al. 1998, MNRAS, 296, 669
Smith, L. J., Crowther, P. A., & Prinja, R. K. 1994, A&A, 281, 833
Smith, L. J., Stroud, M. P., Esteban, C., & Vilchez, J. M. 1997, MNRAS, 290, 265
Smith, M. A., & Balona, L. 2006, ApJ, 640, 491
Smith, N. 2002, MNRAS, 337, 1252
Snow, T. P. 1982, ApJ, 253, L39
Stahl, O., Jankovics, I., Kovács, J., et al. 2001, A&A, 375, 54
Stahl, O., Gäng, T., Sterken, C., et al. 2003, A&A, 400, 279
Stefl, S., Baade, D., Harmanec, P., & Balona, L. A. 1995, A&A, 294, 135
Steiner, J. E., & Damineli, A. 2004, ApJ, 612, L133
Sterken, C. 1977, A&A, 57, 361
Sterken, C., Gosset, E., Juttner, A., et al. 1991, A&A, 247, 383
Sterken, C., Stahl, O., Wolf, B., Szeifert, T., & Jones, A. 1995, A&A, 303, 766
Sterken, C., de Groot, M., & van Genderen, A. M. 1997, A&A, 326, 640
Sterken, C., Arentoft, T., Duerbeck, H. W., & Brogt, E. 1999, A&A, 349, 532
Surdej, J., & Swings, J. P. 1983, A&A, 117, 359
Surdej, A., Surdej, J., Swings, J. P., & Wamsteker, W. 1981, A&A, 93, 285
Thackeray, A. D. 1950, MNRAS, 110, 524
Torrejón, J. M., & Orr, A. 2001, A&A, 377, 148
van der Hucht, K. A. 2001, New Astron. Rev., 45, 135
van Genderen, A. M. 2001, A&A, 366, 508
van Genderen, A. M., Bijleveld, W., & van Groningen, E. 1984, A&AS, 58, 537
van Genderen, A. M., van den Bosch, F. C., Dessing, F., et al. 1992, A&A, 264, 88
van Genderen, A. M., de Groot, M., & Sterken, C. 1997, A&AS, 124, 517
Viotti, R. 1971, PASP, 83, 170
Voors, R. H. M., Waters, L. B. F. M., Trams, N. R., & Kaeufl, H. U. 1997, A&A, 321, L21
Walborn, N. R., & Fitzpatrick, E. L. 2000, PASP, 112, 50
Weis, K., Duschl, W. J., Bomans, D. J., Chu, Y.-H., & Joner, M. D. 1997, A&A, 320, 568
Wolf, B., Campusano, L., & Sterken, C. 1974, A&A, 36, 87
Zorec, J., Frémat, Y., & Cidale, L. 2005, A&A, 441, 235

Online Material

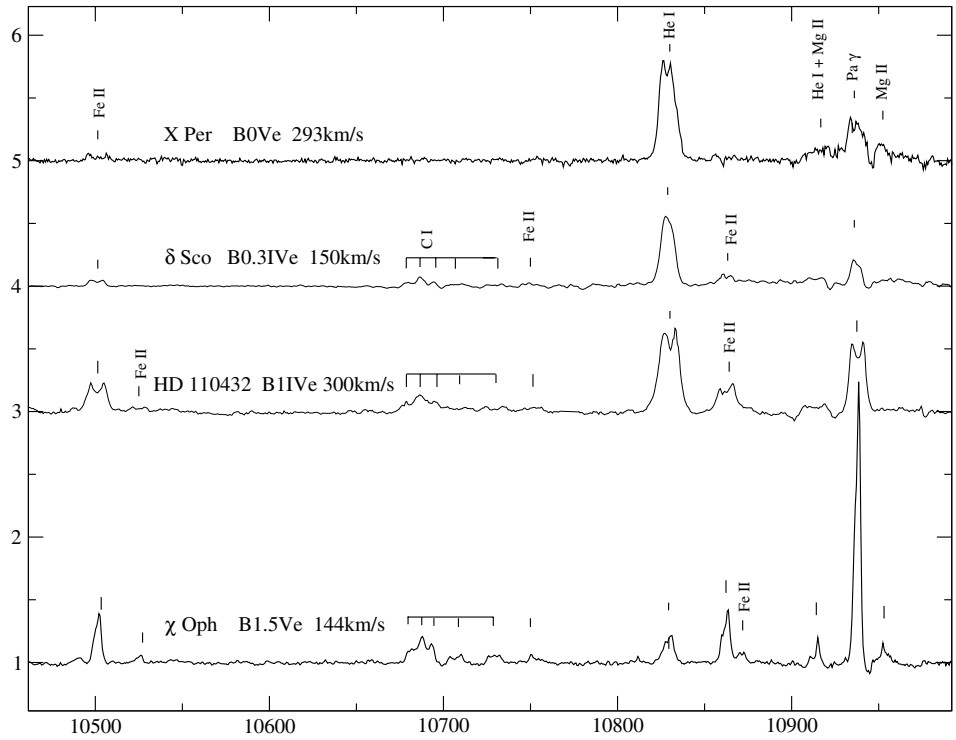

Fig. 5. Spectra of the classical Be stars of our sample ordered by spectral type. Identification, spectral type and projected rotational velocity, respectively, are indicated for each object. From top to bottom, X Per, δ Sco, HD 110432, and χ Oph. For clarity, the spectra were shifted by an arbitrary offset.

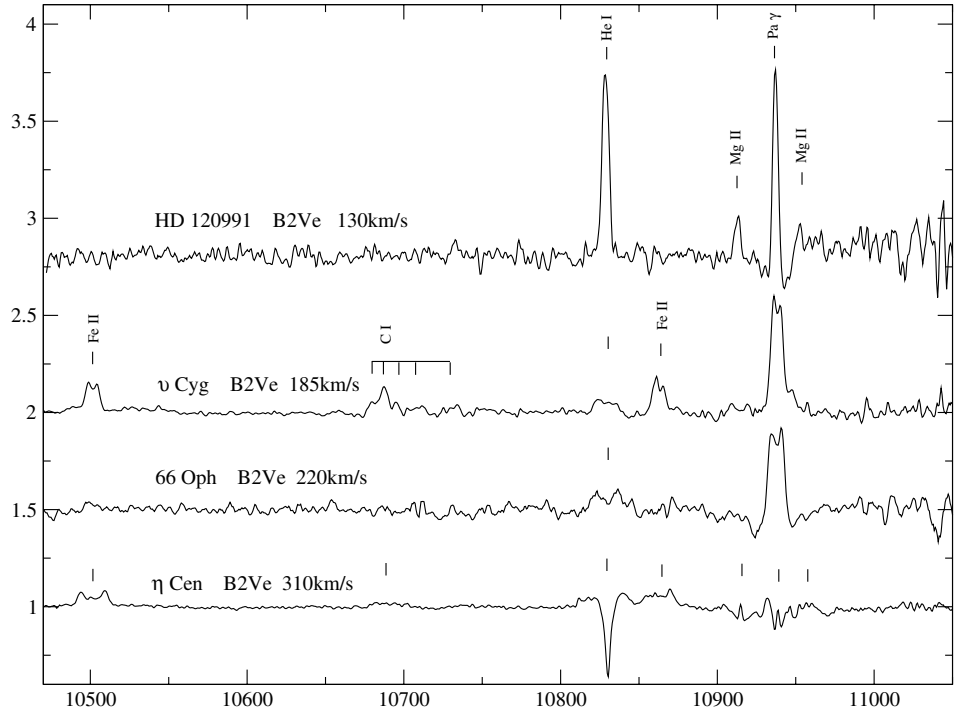

Fig. 6. Same as Fig. 5, showing HD 120991, υ Cyg, 66 Oph, and η Cen.

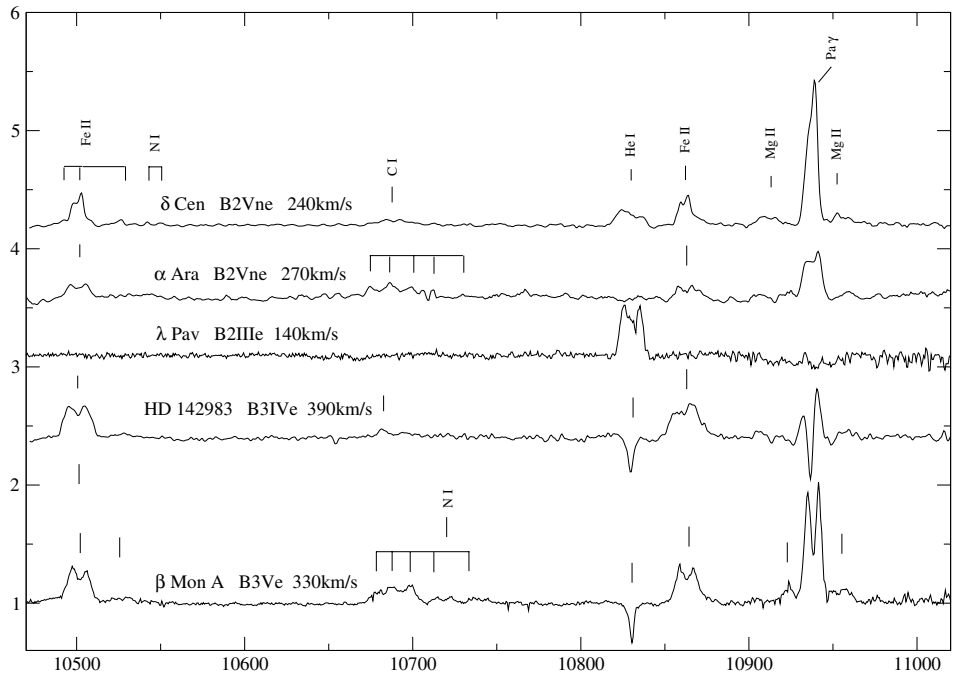

Fig. 7. Same as Fig. 5, showing δ Cen, α Ara, λ Pav, HD 142983, and β Mon A.

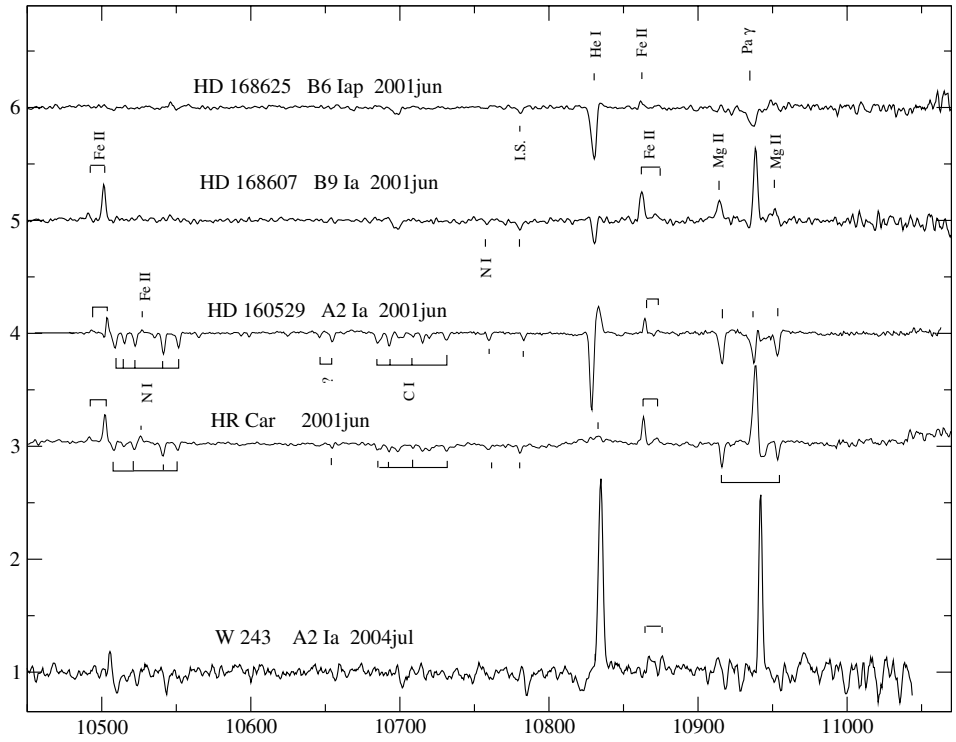

Fig. 8. Spectra of LBVs and LBV candidates. From top to bottom, HD 168625, HD 168607, HD 160529, HR Car, and W243. Spectra of variable stars also give year and month of the observation.

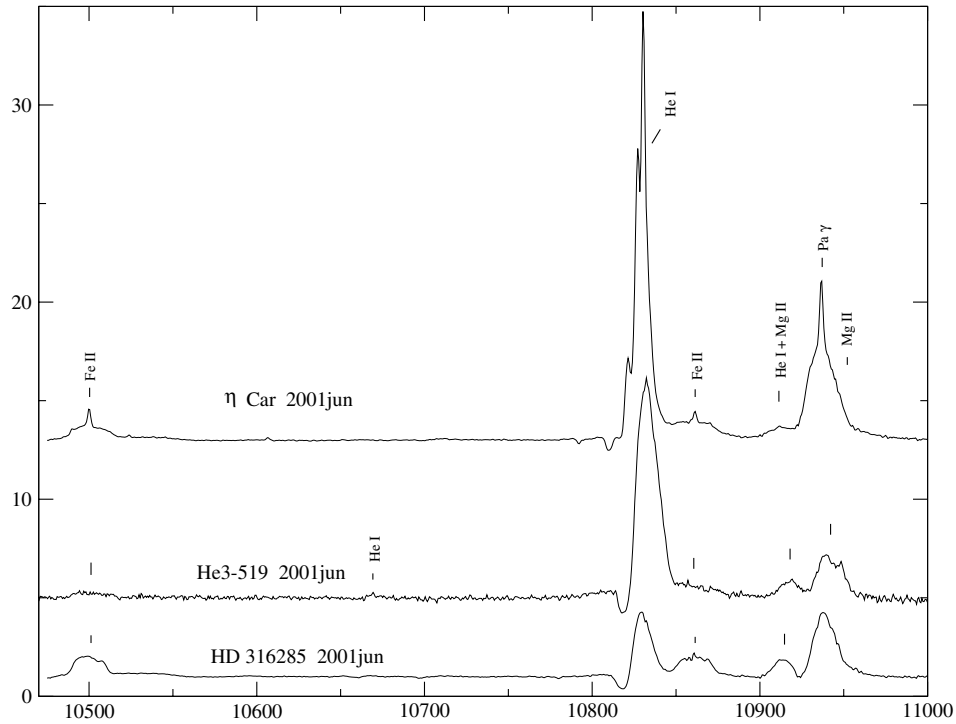

Fig. 9. Same as Fig. 8, showing η Car, He 3-519, and HD 316285.

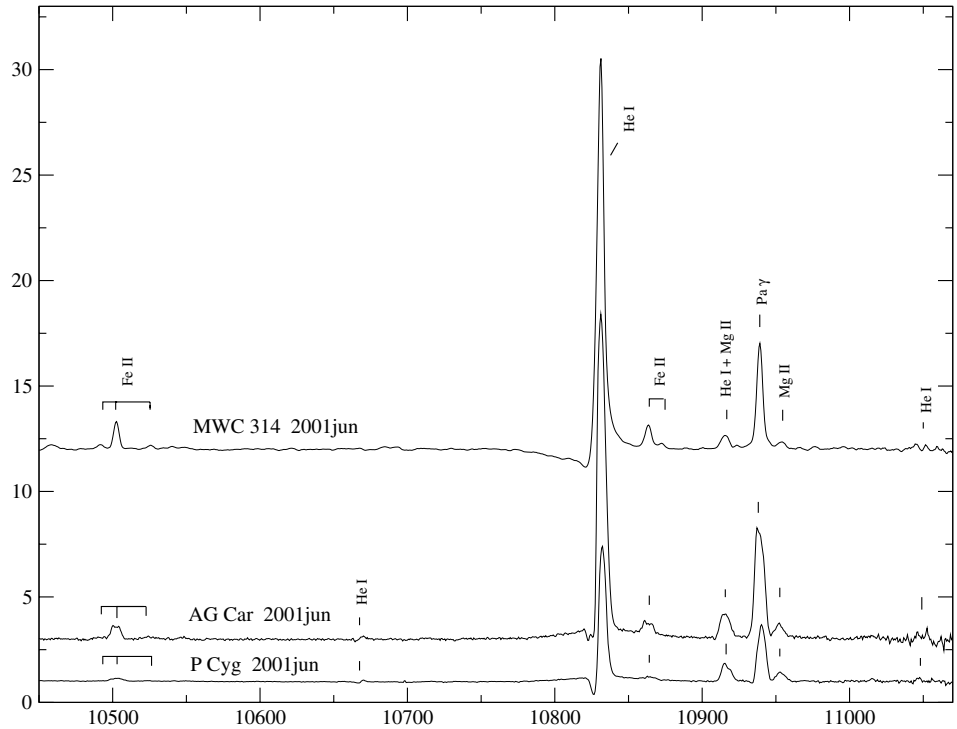

Fig. 10. Same as Fig. 8, showing MWC 314, AG Car, and P Cyg.

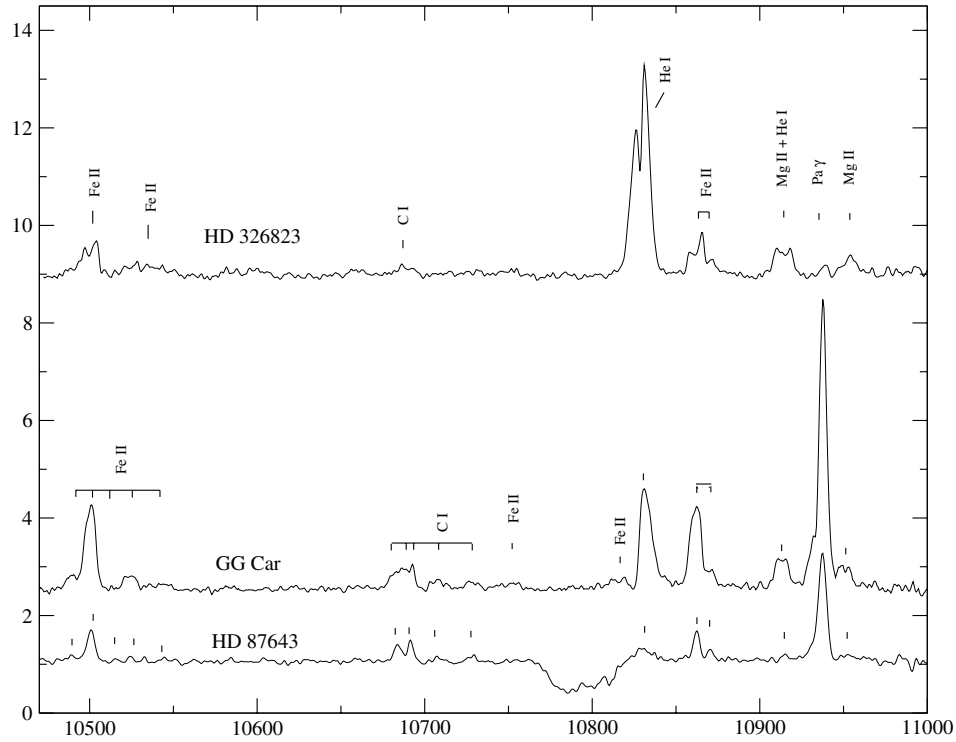

Fig. 11. Same as Fig. 8, showing HD 326823, GG Car, and HD 87643.

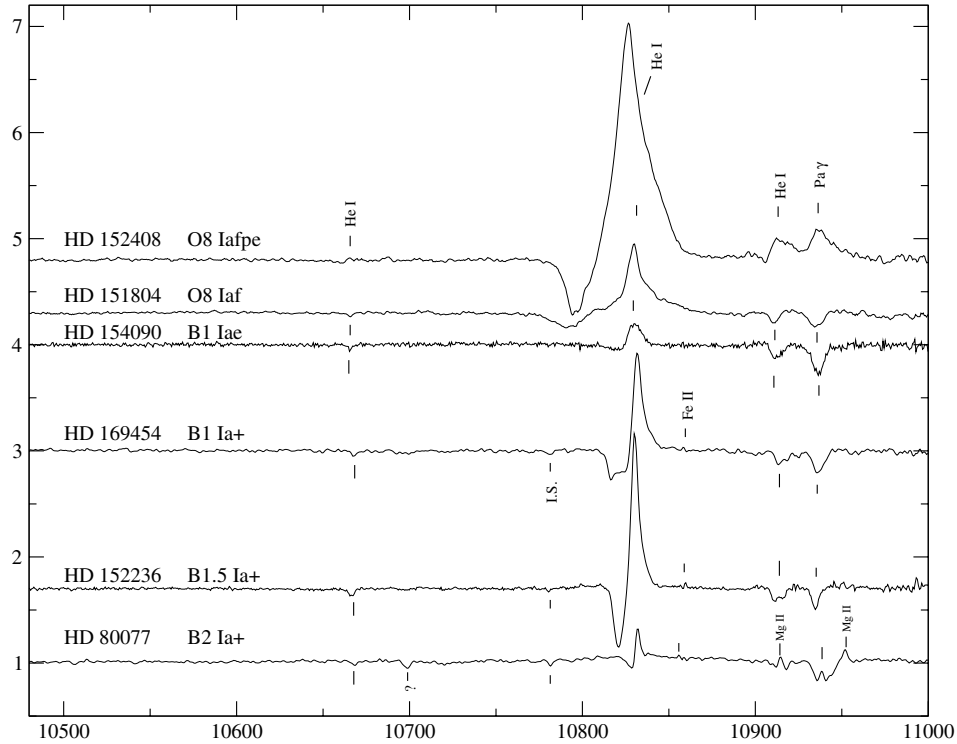

Fig. 12. Spectra of the OB supergiants of our sample, showing from top to bottom HD 152408, HD 151804, HD 154090, HD 169454, HD 152236, and HD 80077. The spectra were offset by an arbitrary offset.

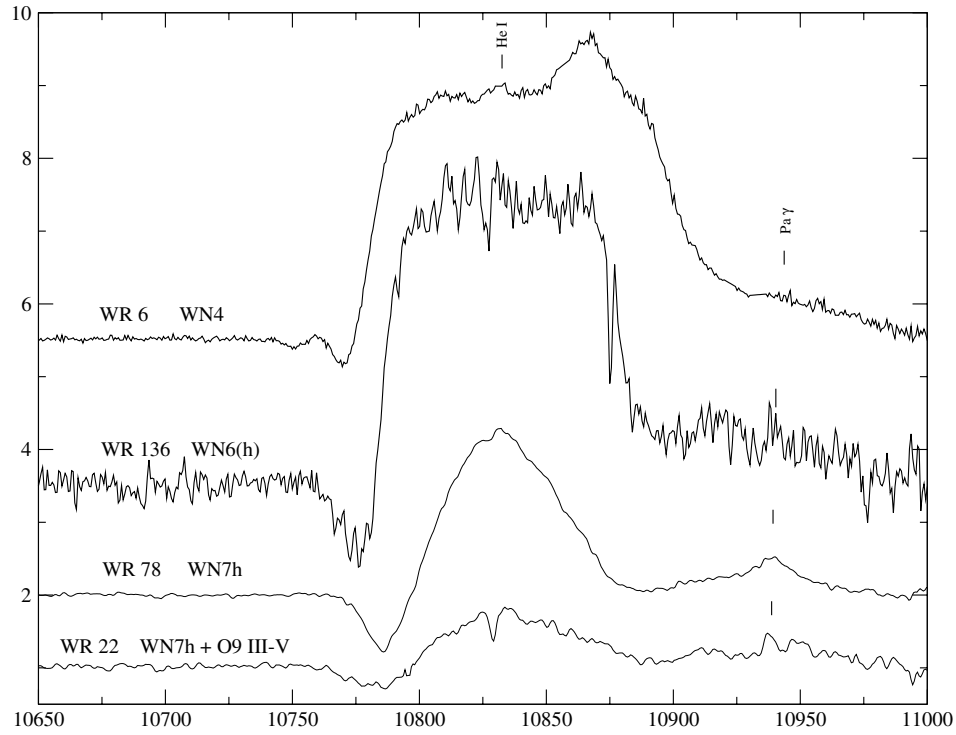

Fig. 13. Spectra of the Wolf-Rayet stars from the WN subtype. From top to bottom, WR 6, WR 136, WR 78, and WR 22.

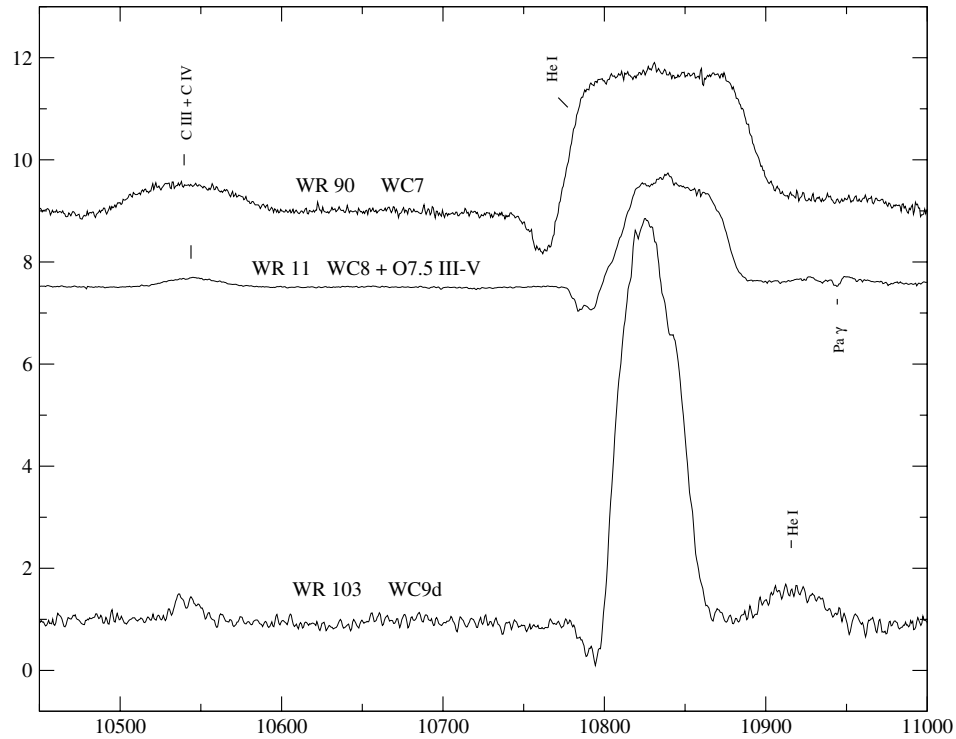

Fig. 14. Same as Fig. 13, but for the Wolf-Rayets of the WC subtype. From top to bottom, WR 90, WR 11 and WR 103.

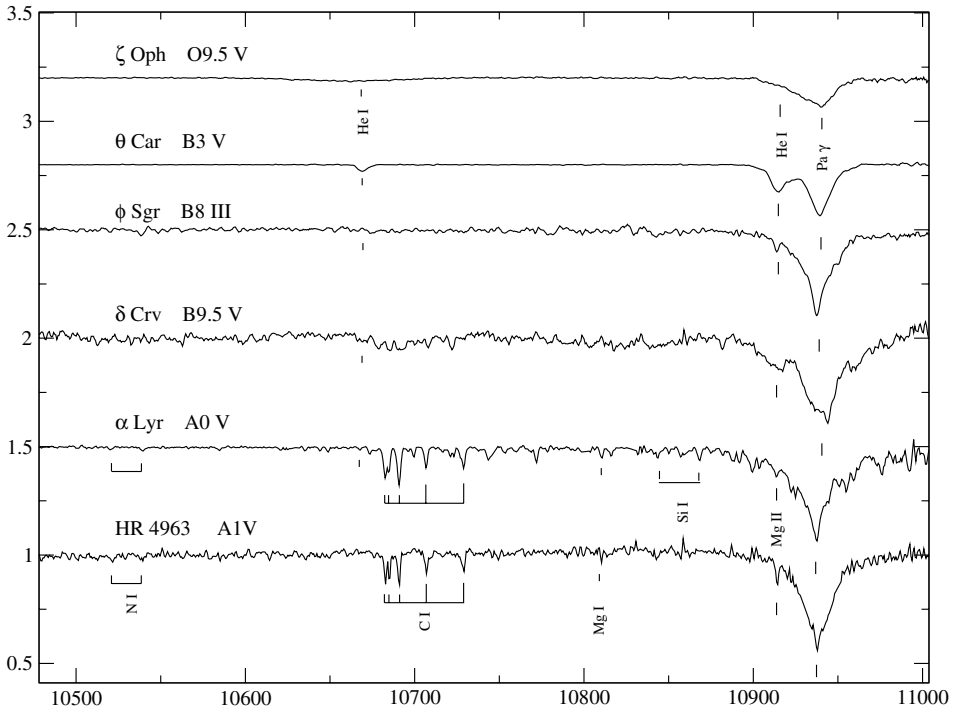

Fig. 15. Spectra of non emission-line early-type stars, showing the typical photospheric lines present in the temperature range of our sample.

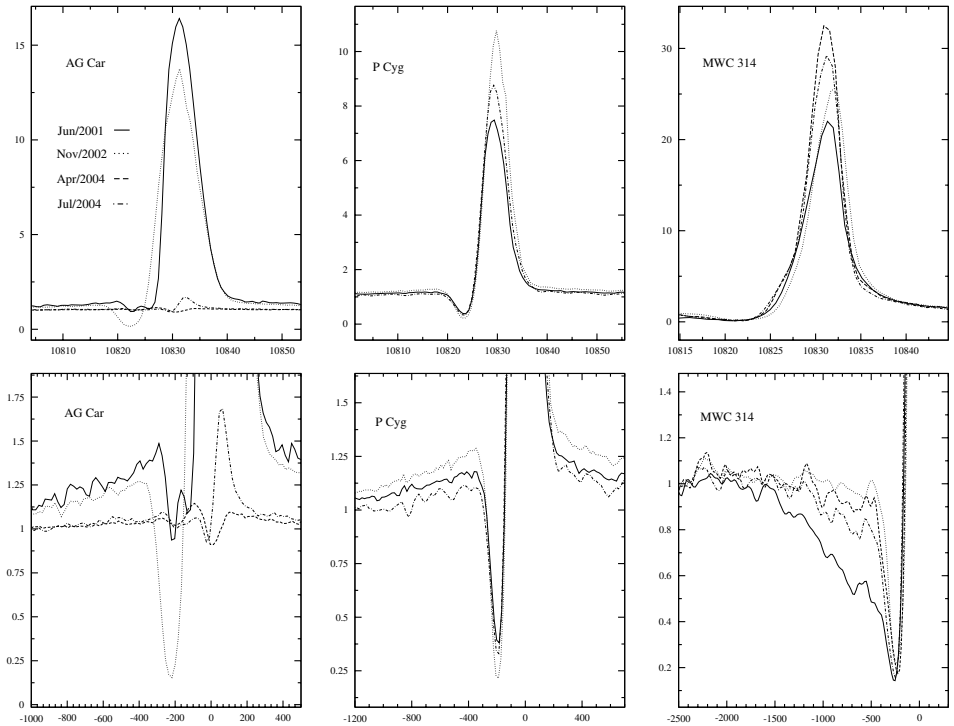

Fig. 16. Spectroscopic variability of LBVs and related objects, from 2001 to 2004 (see legend). *From left to right*, AG Car, P Cyg and MWC 314. For each star, the *upper panel* presents a general view around He I 10 830 Å, while the *lower panel* shows a zoom around the P-Cyg absorption.

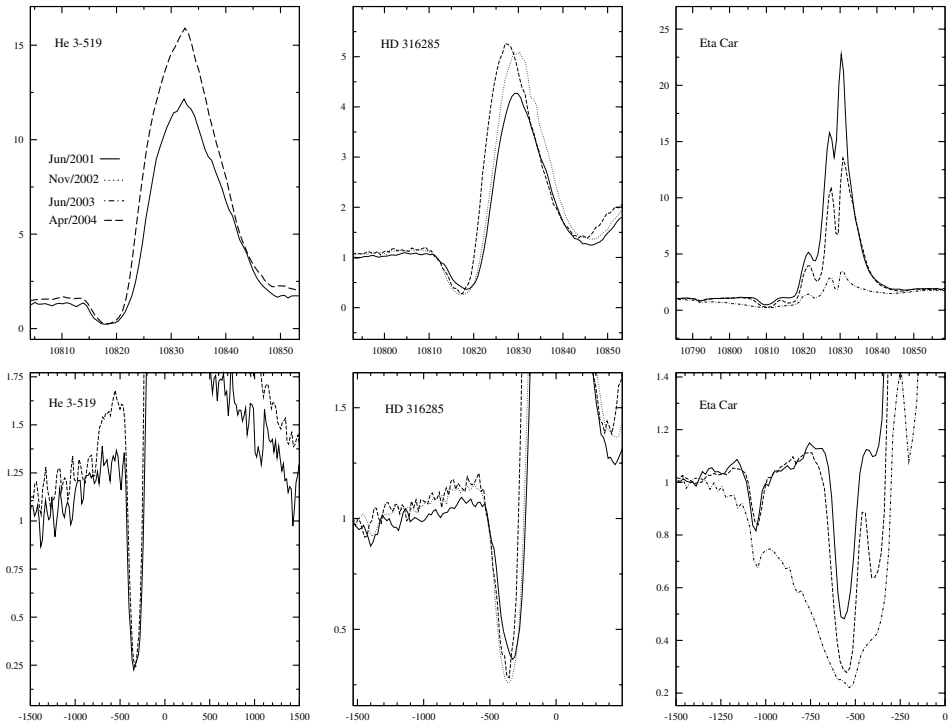

Fig. 17. Same as Fig. 16, but for He 3-519, HD 316285 and η Car.

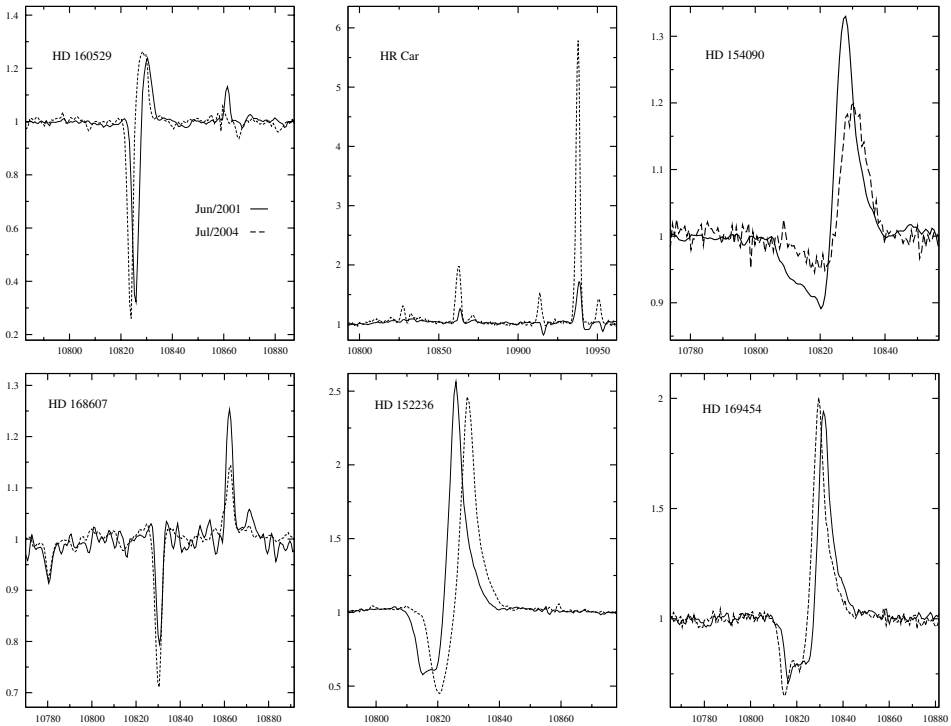

Fig. 18. Same as Fig. 16, but for HD 160529, HR Car, HD 154090, HD 168607, HD 152236 and HD 169454. Note the significant changes in radial velocity of HD 160529, HD 152236 and HD 169454.